UNIVERSITI PUTRA MALAYSIA

EFFECT OF TUNGSTEN OXIDE TO THE STRUCTURAL AND ELASTIC PROPERTIES OF ALUMINA LEAD TELLURITE GLASS SYSTEM (Al2O3-PbO-TeO2)

NUR AQILAH BT SHAARI

EFFECT OF TUNGSTEN OXIDE TO THE STRUCTURAL AND ELASTIC PROPERTIES OF ALUMINA LEAD TELLURITE GLASS SYSTEM

(Al_2O_3-PbO-TeO_2)

By

NUR AQILAH BT SHAARI

196715

Thesis Submitted to the Department of Physics, Universiti Putra Malaysia, in partial Fulfilment of the Requirement for the Degree of Bachelor of Science with Honours in Material Science

February 2022

DEDICATION

To my beloved parents Mr Shaari bin Md. Yusoff and Mrs Hamidah binti Abdul Rahman

For their unconditional love and support

To my beloved siblings and family

For their support and love

To all of my precious friends

For the thick and thin we had been together and makes my life full of excitements

To all my lectures

For helping me throughout this journey and teach me lots of things

Thank you all

ABSTRACT

EFFECT OF TUNGSTEN OXIDE TO THE STRUCTURAL AND ELASTIC PROPERTIES OF ALUMINA LEAD TELLURITE GLASS SYSTEM (Al_2O_3-PbO-TeO_2)

By

NUR AQILAH BINTI SHAARI

(196715)

February 2022

Supervisor : Dr. Mohd Hafiz Mohd Zaid

Department : Physics, Faculty of Science

The production of tungsten oxide alumina lead tellurite glasses at different compositions added according to the empirical formula $x(WO_3)$-5(Al_2O_3)-15(PbO)-80-x(TeO_2) with x = 0, 5, 10, 15, and 20 mol % were prepared by using the melt quenching technique and investigated by XRD, ultrasonic velocities, density, molar volume, and the properties of structural and elastic model. The physical parameters of the glasses were determined by density and molar volume using the Archimedes method, while the elastic properties were determined by XRD and ultrasonic velocities. XRD confirmed the amorphous WO_3- Al_2O_3-PbO-TeO_2 glass structure, a broad halo peak at a lower angle ≈ 20°- 27° and continuous sharp peak not found were observed in glass system. From the density measurement, the addition of WO_3 observed has increase the density from 6.232 to 6.847 g/cm^3 and the molar volume decreased from 26.68 to 26.44 cm^3/mol of the glasses. In addition, the OPD is increased from 71.22 to 79.57 mol/cm^3. The elastic properties approximated from measured shear (V_S) and longitudinal (V_L) ultrasonic velocities increased from 1600 to 1813 cm^{-1} and from 2823 to 3289 cm^{-1}, when WO_3 content increased from 0 to 20 mol%. Meanwhile, the longitudinal (L), shear (G), bulk (K) and Young's

(E) modulus increased from 49.66 to 74.07 GPa, 15.95 to 22.51 GPa, 28.39 to 44.06 GPa and 40.19 and 57.63 GPa, respectively. The Poisson's ratio also increased from 0.263 to 0.282 and micro hardness increased from 2.514 to 3.267 GPa. Estimated parameters based on Makishima–Mackenzie theory and Rocherulle theory calculated in order to analyse the correlation between them. Makishima–Mackenzie model, the longitudinal (L_m), shear (G_m), bulk (K_m) and Young's (E_m) modulus increased from 25.27 to 27.31 GPa, 8.75 to 9.88 GPa, 10.67 to 12.06 GPa and 23.15 and 26.54 GPa. Besides, the values of micro hardness (H_m) and Poisson's ratio (σ_m**)** also increased from 1.18 to 3.11 GPa and 0.219 to 0.247. For Rocherulle model, longitudinal (L_r), shear (G_r), bulk (K_r), Young's (E_r) modulus increased from 34.01 to 36.83 GPa, 9.95 to 11.32 GPa, 13.21 to 14.76 GPa and 20.26 to 23.94 GPa. Similarly, the micro hardness (H_r) and Poisson's ratio (σ_r) also increased from 1.04 to 2.12 GPa and 0.284 to 0.410. The results of XRD, ultrasonic velocities and elastic moduli evidenced the formation of WO_3-Al_2O_3-PbO-TeO_2 glass system and potentially used in the fields of photonics as laser diode.

KESAN TUNGSTEN OKSIDA TERHADAP SIFAT STRUKTUR DAN ELASTIK DARIPADA SISTEM KACA ALUMINA PLUMBUM TELLURITE

Oleh

NUR AQILAH BINTI SHAARI
(196715)

Februari 2022

Penyelia: Dr. Mohd Hafiz Mohd Zaid

Fakulti: Fakulti Sains

Penghasilan kaca tellurite plumbum tungsten oksida alumina pada komposisi berbeza yang ditambah mengikut formula empirik $x(WO_3)$-$5(Al_2O_3)$-15(PbO)-80-$x(TeO_2)$ dengan x = 0, 5, 10, 15, dan 20 mol % telah disediakan dengan menggunakan teknik pelindap kejutan leburan dan disiasat oleh XRD, halaju ultrasonik, ketumpatan, isipadu molar dan sifat-sifat model struktur dan keanjalan. Parameter fizikal kaca ditentukan oleh ketumpatan dan isipadu molar menggunakan kaedah Archimedes, manakala sifat keanjalan ditentukan oleh XRD dan halaju ultrasonik. XRD mengesahkan struktur kaca WO_3- Al_2O_3-PbO-TeO_2 amorfus, puncak halo luas pada sudut yang lebih rendah ≈ 20°- 27° dan puncak tajam berterusan yang tidak ditemui diperhatikan dalam sistem kaca. Daripada pengukuran ketumpatan, penambahan WO_3 yang diperhatikan telah meningkatkan ketumpatan daripada 6.232 kepada 6.847 g/cm^3 dan isipadu molar menurun daripada 26.68 kepada 26.44 cm^3/mol kaca. Di samping itu, OPD dinaikkan daripada 71.22 kepada 79.57 mol/cm^3. Sifat keanjalan yang dianggarkan daripada halaju ultrasonik ricih (VS) dan longitudinal (VL) yang diukur meningkat daripada 1600 kepada 1813 cm-1 dan dari 2823 kepada 3289 cm-1, apabila kandungan WO_3 meningkat daripada 0 hingga

20 mol%. Sementara itu, modulus longitudinal (L), ricih (G), pukal (K) dan Young (E) masing-masing meningkat daripada 49.66 kepada 74.07 GPa, 15.95 kepada 22.51 GPa, 28.39 kepada 44.06 GPa dan 40.19 dan 57.63 GPa. Nisbah Poisson juga meningkat daripada 0.263 kepada 0.282 dan kekerasan mikro meningkat daripada 2.514 kepada 3.267 GPa. Parameter anggaran berdasarkan teori Makishima–Mackenzie dan teori Rocherulle dikira untuk menganalisis korelasi antara mereka. Model Makishima–Mackenzie, modulus membujur (Lm), ricih (Gm), pukal (Km) dan Young (Em) meningkat daripada 25.27 kepada 27.31 GPa, 8.75 kepada 9.88 GPa, 10.67 kepada 12.06 GPa dan 23.15 dan 26.15 dan GPa. Selain itu, nilai kekerasan mikro (Hm) dan nisbah Poisson (σm) juga meningkat daripada 1.18 kepada 3.11 GPa dan 0.219 kepada 0.247. Untuk model Rocherulle, modulus membujur (Lr), ricih (Gr), pukal (Kr), modulus Young (Er) meningkat daripada 34.01 kepada 36.83 GPa, 9.95 kepada 11.32 GPa, 13.21 kepada 14.76 GPa dan 20.26 kepada 23.94 Begitu juga, kekerasan mikro (Hr) dan nisbah Poisson (σr) juga meningkat daripada 1.04 kepada 2.12 GPa dan 0.284 kepada 0.410. Keputusan XRD, halaju ultrasonik dan moduli elastik membuktikan pembentukan sistem kaca WO_3- Al_2O_3-PbO-TeO_2 dan berpotensi digunakan dalam bidang fotonik sebagai diod laser.

ACKNOWLEDGEMENTS

In the name of Allah S.W.T, the Most Gracious and Most Merciful. I am very grateful to Allah for the blessing to be able to complete my thesis. First and foremost, special appreciation goes to my supervisor, Dr. Mohd Hafiz bin Mohd Zaid, for his supervision, continue guidance, helpful ideas and valuable advice on my project throughout my research period. Throughout the experimental and thesis works, his invaluable aid of insightful comments and recommendations has led to the success of this study. Besides, my sincere gratitude for their encouragement and patience during my study to my seniors, Wei Mun and Zhi Wei. They never hesitated to help, share their ideas and opinions of experimental and thesis work. I also want to thank my partner Nur Hidayah for her invaluable discussion and for the entire research work of her patient and sincerity. Not forgotten to my final year project members and friends who assist me in doing this research throughout the journey. All staff and technicians from the Faculty Of Science are also humbly appreciated for the cooperation and technical support offered. Lastly, my heartfelt appreciation goes to my parents, Mr. Shaari bin Md. Yusoff and Mrs. Hamidah binti Abdul Rahman for their constant love, prayers and support. In completing this report, may Allah bless all the people for giving me the utmost support.

TABLE OF CONTENT

LIST OF TABLES

LIST OF FIGURES

LIST OF ABBREVIATIONS

XRD	X-ray Diffraction
WO_3	Tungsten Trioxide
Al_2O_3	Aluminum Oxide
PbO	Lead Oxide
TeO_2	Tellurium Dioxide
TiO_2	Titanium Dioxide
WO_4	Tungstate
V_2O_5	Vanadium Pentoxide
Te^{4+}	Tellurium

CHAPTER 1

INTRODUCTION

1.1 Research background

Glass, an inorganic solid material that is usually transparent or translucent as well as hard, brittle, and impervious to the natural elements. Additionally, glass may be characterised as an amorphous material that can be formed by the use of melt-quenching processes (Çelikbilek et al., 2013). Glasses formed using melt-quenching processes may experience certain thermal effects, which will impact their stability, diffusivity, relaxation time, and position of the glass transmission temperature (Hilden & Morris, 2004). FT-IR spectroscopy, density measurements, and quantum chemical computations were used to explore the structural features of many tellurite glasses (Rada et al., 2009).

As lead glass, colloquially referred to as crystal, is a type of glass in which lead is used in place of calcium in a conventional potash glass. Lead glass normally includes between 18 to 40% lead (II) oxide, but modern lead crystal, formerly referred to as flint glass due to its silica source, includes at least 24% PbO. Glass has certain unique features, such as great hardness and transparency at room temperature, as well as enough strength and great corrosion resistance. The study of the characteristics of glasses is of tremendous importance vmaterials offer well-known benefits such as physical isotropy, the lack of grain boundaries, and the ability to be employed for optical applications. Tellurium oxide, TeO_2, is a conditional glass former that requires a modifier ion to readily create the glassy state. It is also well-known for having important features such as a high refractive index, a low phonon

maximum, a low melting temperature, and a high dielectric constant. The longitudinal, shear, Young's, and bulk moduli of structural and elastic models were found using the Poisson's ratio. Makishima and Mackenzie and Rocherulle proposed that the elastic moduli of oxide glasses take into consideration the energy dissociation per unit volume (G_t) and packing density (V_t). Given the above, the purpose of this work is to determine the influence of tungsten trioxide on the structural and elastic characteristics of an alumina lead tellurite glass system. Numerous papers have been devoted to the study of tellurite glasses' many features (ranging from structural, elastic, mechanical, optical, and spectroscopic characteristics) in recent years owing to its apparent advantage over other glasses in a variety of technological applications. This is shown by the fact that the TeO2 composition of glasses is used to achieve a high refractive index, ease of production, high transmittance in the infrared region, strong optical nonlinearity, and low phonon energies (Sio et al., 1997). A thorough investigation of the crystallisation, characteristics, and impacts of tungsten trioxide on alumina lead tellurite glass was conducted, as well as the application of the glass and the measurement findings (Nazrin et al., 2018).

1.2 Problem Statement

Tellurium (TeO_2) is a conditional glass maker and the use of a twin roller method to quickly cool down has reduced the production of glass. Most glass-forming oxides have a number that is entire and a glass-like structure comparable to the crystalline structure. In the beginning it was believed that tellurium dioxide was likewise following this trend, however this seems to be not the case according to neutron dispersion and Raman spectroscopy (Hauke et al., 2018). In addition, pure TeO_2 glass is not stable and can be readily crystallised since the lone pair of electrodes is present at TeO_4 equatorial position, severely restricting

the structural reorganisation of the units required for the production of glass. The inclusion of a modest number of modifier oxides such as WO_3, however, makes TeO2 a highly excellent glass-former (Fares et al., 2014). Al_2O_3 is incapable of forming a glass on its own. When combined with other appropriate oxides, it may produce glass and contribute to the creation of the glass structural unit (Pal Singh et al., 2011).

1.3 Objectives

The primary purpose of this project is to investigate the effect of tungsten trioxide on the structural and elastic characteristics of the alumina lead tellurite glass system. The primary procedures involved in the creation of alumina lead tellurite glass were melt quenching, the addition of WO_3, and the analysis of XRD, density, molar volume, ultrasonic velocities, and the structural and elastic characteristics of the glass.

There are several specific objectives in this analysis as in the following:

1. To synthesize tungsten alumina lead tellurite glass system using conventional melt-quenching method.
2. To study the effect of WO_3 to the structural and elastic properties of alumina lead tellurite glass system.
3. To investigate the correlation between Makishima and Mackenzie model and the Rocherulle model to the elastic properties of tungsten alumina lead tellurite glass system.

1.4 Scopes of the study

There are some scope of study as follows :-

1) Glass preparation using some raw material such as WO_3, Al_2O_3 , PbO and TeO_2 powder based using empirical formula $x(WO_3)$-5(Al_2O_3)-15(PbO)-80-$x(TeO_2)$ (x = 0, 5, 10, 15 and 20 %) by melt-quenching technique.

2) Analyze structural and elastic properties of WO_3-Al_2O_3-PbO-TeO_2 glass samples using XRD , FTIR , ultrasonic velocities and Makashima and Meckenzie model.

1.5 Outline of the thesis

Each chapter has a well-organized series of investigations. Each chapter has been adequately created, with a thesis statement that aids in the organisation of ideas. The first chapter examines the history of the tellurite glass issue, the introduction of lead tellurite glass, the problem statements, the objective of the research, and the relevance of this research. Chapter 2 provided an overview of structural and elastic investigations. Additionally, it discussed the glass structure and behaviour of tungsten trioxide when combined with alumina lead tellurite glass. The glass forming system has been thoroughly explored. Additionally, the structural and elastic characteristics will be discussed. Chapter 3 details the methodological procedures involved in the manufacture of glass, as well as the methodologies utilised to analyse the numerous spectroscopic data associated with structural attributes. The precursor glass and alumina lead tellurite glass with tungsten trioxide addition are described in detail, as well as the methods and characterization.

CHAPTER 2

LIRATURE REVIEW

2.1 Introduction

This chapter 2 provides an in-depth examination of glass. To begin, there is a dearth of studies examining the effect of WO_3 on alumina lead tellurite glass. Additionally, tellurite glass was examined. The glass, which is composed of alumina lead tellurite and tungsten trioxide, was thoroughly reviewed. This chapter concludes with a description of the elastic modelling techniques that were utilised to determine the elastic parameters in this study.

2.1.1 Glass

Glass is an inorganic solid that is often transparent or translucent, as well as hard, brittle, and resistant to the elements. While glass may have a wide variety of chemical compositions, the majority of formulations exhibit the following properties which are transmits visible light: Glass is typically transparent to the electromagnetic spectrum's visible part. However, the surface of glass scatters or reflects light, and the material is brittle, resistant to chemical assault, pourable, shaped, moulded, and extruded, with a potential for high tensile strength (Anne Marie Helmenstine, 2019). Glass production occurs in a wide variety of chemically different materials, including covalent, ionic, molecular, metallic, and hydrogen-bonded compounds. Elements, simple chemical compounds, complex organic molecules, salt combinations, and alloys have all been used to make glasses. There is no especially beneficial method to classify materials used in the manufacture of glass. Goldschmidt (1926) made the first attempt to link glass formation to structure, recognising the significance of radius ratios in simple glass producing

oxides. From the past research, can be noted that r_c/r_o is 0.2 to 0.4 in all glass producing oxides known at the time, where r_c and r_o are the cation and anion, ionic radii, respectively (Bragg, 2002). Zachariasen published the first paper on these components in 1932, and it is considered a seminal work in the field of glass research. The discussion of the ideas on glass and categorises the three kinds of cations found in glass networks: network formers, network modifiers, and intermediates (Grayson, 2020).

2.1.2 Glass Former

The composition of glass determines its characteristics. One of the most important compositional modifications that may be made is to the glass's fundamental unit: the network former. The former may be regarded of as the glass's backbone, and altering this element or compound significantly affects the final material's characteristics. Glass formers are introduced to the bulk material to enhance the development of a glass and to create the glass network's linked backbone. In network formers some frequent cations include boron, silicone, germanium, and phosphorus. They are of high valence (that means they have an electron excess or deficiency that allows them to readily bind with other atoms) and bind them covalently to oxygen. Added network ions that modify the glass network and intermediates to get unique glass characteristics. Numerous glass formers are combined in various proportions with modifiers and intermediates to create a glass that is capable of withstanding the demands of a particular application. For instance, a glass designed to handle hot liquids will have a different composition than one designed for decorative purposes (Grayson, 2020). Tellurium dioxide (TeO_2) is a conditional glass former, and fast cooling through the twin roller method has allowed limited glass formation. (Hauke et al., 2020).

2.1.3 Glass Intermediate

Intermediate glasses have almost constant elastic moduli as a function of temperature and pressure. These glasses would be advantageous for developing a thermal optical fibres for improved telecommunications and fibre sensing applications, as well as for developing glass products for applications involving a wide spectrum of thermal and mechanical stimulation (Jaccani et al., 2018). Intermediates, which include titanium, aluminium, and zinc, are compounds that, depending on the glass composition, act as network-formers or modifiers. Glasses are intrinsically extremely disordered materials that need a precise balance of network formers, intermediates, and modifiers to avoid the development of ordered crystallites inside the material (Grayson, 2020). The oxides are referred to as intermediates because they, like network modifiers, decrease the glass's melting point and viscosity, enabling it to be worked at lower temperatures. TiO_2, ZnO, PbO, and Al_2O_3 are all examples of common intermediates.

2.1.4 Glass Modifier

Modifiers are substances that may be applied in trace amounts to glass to further change its characteristics. These elements include lithium, sodium, potassium, and calcium; they reside as charged single atoms (ions) inside the cross-linked network formers, decreasing the glass's relative number of strong bonds and therefore its melting point and viscosity. By weakly interacting with oxygen atoms, glass modifiers disrupt the usual bonding between glass-forming components and oxygen. This results in the formation of "non-bridging oxygens" and

a decrease in the quantity of strong bonding inside the glass. As a consequence, glass modifiers have a noticeable impact on the characteristics of glass. These include a decrease in melting temperature, surface tension, and viscosity as a result of the material's overall bonding being weaker (Grayson, 2020). Glass modifiers may further transform glass into a genuine wonder-material. The characteristics of glass may be precisely adjusted and enhanced, much as with other materials such as steel, by carefully adding chemical modifiers to suit a wide variety of demanding applications.

2.2 Tellurite Glass

Tellurium oxide (TeO_2) is the primary constituent of tellurite glasses. Tellurium dioxide is referred to be a conditional glass former, and as such requires a modifier to create the glassy state readily (Mustafa et al., 2013). Tellurium dioxide (TeO_2), with a melting point of 733°C, is the most stable oxide of tellurium (Te) (Dutton and Cooper 1966). The stability qualities of tellurium oxides were shown to be transferable to their glass derivatives, allowing for experimentation with a broader range of components in the composition of tellurite glasses and therefore better control over performance characteristic variation (El-Mallawany & El-Mallawany, 2014). A research of tellurite glasses was deemed worthwhile not just for its intrinsic value, but also because it might be anticipated that these glasses would possess useful physical characteristics. For example, based on the known cation radius of Te^{4+} (0.84 A. in its oxide), one could estimate that the partial refractivity of tellurium oxide (TeO_2) in glass is quite high, and that tellurite glasses thus have much higher refractive indices than corresponding silicate, borate, phosphate, and germanate glasses (Stanworth, 1952). The longitudinal V and shear V velocities of ultrasonic waves propagating through TeO_2 were measured using the

pulse echo overlap method at room temperature. X- and Y-cut quartz transducers were used to produce and receive ultrasonic pluses at a frequency of 10 MHz (El-Mallawany, 1998).

2.3 Lead Tellurite Glass

The produced glass samples were homogenous and lime green in colour, becoming more transparent as the PbO concentration increased. The XRD pattern verified the two glass systems' amorphous character. The FTIR spectrum of the binary glass system revealed a reduction in the concentration of non-bridging oxygen (NBO) with the addition of PbO, which subsequently increased when additional PbO was added to the system. The addition of PbO to the binary results in an increase in density, but a reduction in molar volume in the tellurite glass system (Alazoumi, 2018). When transition metal oxides (TMOs) are added to binary vanadate tellurite glasses, the glass network undergoes structural rearrangement (Palanivelu & Rajendran, 2006).

2.4 WO_3 added in Tellurite glass

Tungsten oxide is a highly sought-after material that has been widely studied for its unique characteristics. The tungsten ion occurs in a variety of valence states, including $W^{6+,}$ W^{5+}, and $W^{4+.}$ As a result, its doping has the potential to alter the structure and optical characteristics of host glasses. The WO_3 are network conditional formers. Another factor contributing to the increased density of glasses is the presence of tungsten ions with structural groups WO_4 or WO_6 in the glass network. Due to the fact that WO_3 is more polarizable than Al_2O_3, these

elements contribute to the increased density of the glass system. The rise in density indicates the compression of the glass structure as the WO_3 concentration increases (Pal Singh et al., 2011). According to the literature, it is possible to enhance or preserve the linear and nonlinear optical indices of TeO_2 based glasses by adding transition-metal oxides, such as tungsten oxide WO_3. This process is referred to as 'structural depolymerization' of the TeO_2 rich network because it reduces the crosslinking density of the network by breaking the Te-O-Te bridges (Zaki et al., 2019).

2.5 Elastic moduli model

The Makishima–Mackenzie (MM) model estimates the Young's modulus of glass from its composition and component characteristics. This model is often used to predict the stiffness of glass and to link results with composition (Plucinski & Zwanziger, 2015). Several simplified theoretical models have been developed in recent years to determine the elastic moduli and Poisson's ratio of simple and multicomponent oxide glasses based on their chemical compositions. Among these models, the one that is most commonly used is Makishima & Mackenzie's, which was later improved by Rocherulle et al. Recent work by the author and colleagues has concentrated on predicting the elastic characteristics of vanadate and V_2O_5 contained tellurite, borate, and phosphate glass systems using Makishima–theory, Mackenzie's the Rocherulle et al model, and other methods in the area. For the majority of the V_2O_5 containing glass systems investigated, there was a discrepancy between theoretical and experimental elastic moduli. This discrepancy has been ascribed to the glass's atypical behaviour (inverse proportionality) between elastic moduli and estimated dissociation energy per unit volume. The anomalous relationship between elastic moduli and glass dissociation energy per unit volume has been rectified by considering the impact of the two fundamental

structural units VO_4 and VO_5 on the glass's dissociation energy per unit volume. The remarkable concordance between theoretical and experimental elastic moduli demonstrates this (Abd El-Moneim, 2019).

CHAPTER 3

METHODOLOGY

3.1 Introduction

This chapter was written to explain how to make tungsten alumina lead tellurite glass. The glass was made using the melt-quenching technique, which is a traditional method for making glass that involves mixing the ingredients and quenching the glass melt to create a glass. However, alumina lead tellurite glass was formed as a result of the densification and crystallisation processes. In addition, this chapter presents measurements from a variety of techniques on glass samples, XRD, density, molar volume, ultrasonic velocities, elastic modulus, Makishima and Mackenzie model, and Rocherulle model. The physical, structural, and elastic properties of the glass were analysed on the glass samples.

3.2 Sample preparation

The melt-quenching process is a well-established method for creating glasses. However, this process is employed to manufacture glassy materials since it allows for the investigation of new oxide glasses and the quick formation of glass. Typically, the glass utilised has some unique properties, such as a low melting point, a strong resistance, a vast region of glass production, and a higher refractive index. Because the quenching process is one of the most precise and difficult to control, cooling must occur quickly. Thus, precautions must be made during the chilling process to avoid crystallisation, which occurs when new crystals phase

apart and then develop to bigger sizes. Both of these processes are referred to as nucleation and crystallisation.

In this study, tungsten trioxide, WO_3, aluminium oxide, Al_2O_3, lead monoxide, PbO and tellurium oxide, TeO_2 are used as the raw materials to prepare the glass. The WO_3, Al_2O_3, PbO and TeO_2 was weighed using a digital analytical balance to prepare a series of glasses sample based on the empirical formula $x(WO_3)$-5(Al_2O_3)-15(PbO)-80-$x(TeO_2)$ (x = 0, 5, 10, 15, and 20 mol %) with the total weight of 30g for each glass. The analytical balance has the accuracy of ± 0.1 mg. The compositions of each glass based on the empirical formula is shown in **Table 3.1.**

Table 3.1 The compositions of each $x(WO_3)$-5(Al_2O_3)-15(PbO)-80-$x(TeO_2)$ glasses.

Glass sample	**Molar Percentage (mol %)**			
	WO_3	**Al_2O_3**	**PbO**	**TeO_2**
G1	0	5	15	80
G2	5	5	15	75
G3	10	5	15	70
G4	15	5	15	65
G5	20	5	15	60

After weighing and mixing, the powder combination was deposited in the crucible and then placed in the electric furnace to melt at 950 °C for approximately 3 hours. The crucible was then carefully removed from the electric furnace using long crucible tongs and cast into a rectangular mould that had been preheated to 250 °C for approximately 1 hour. To avoid shattering the glass mass, the sample was placed in an annealing furnace set to 350°C for

approximately 1 hour and then progressively cooled to ambient temperature. These samples were cut and will next be polished and ground in order to determine the glass samples for its characteristics. **Figure 3.1** shown the main process of preparing the glass samples.

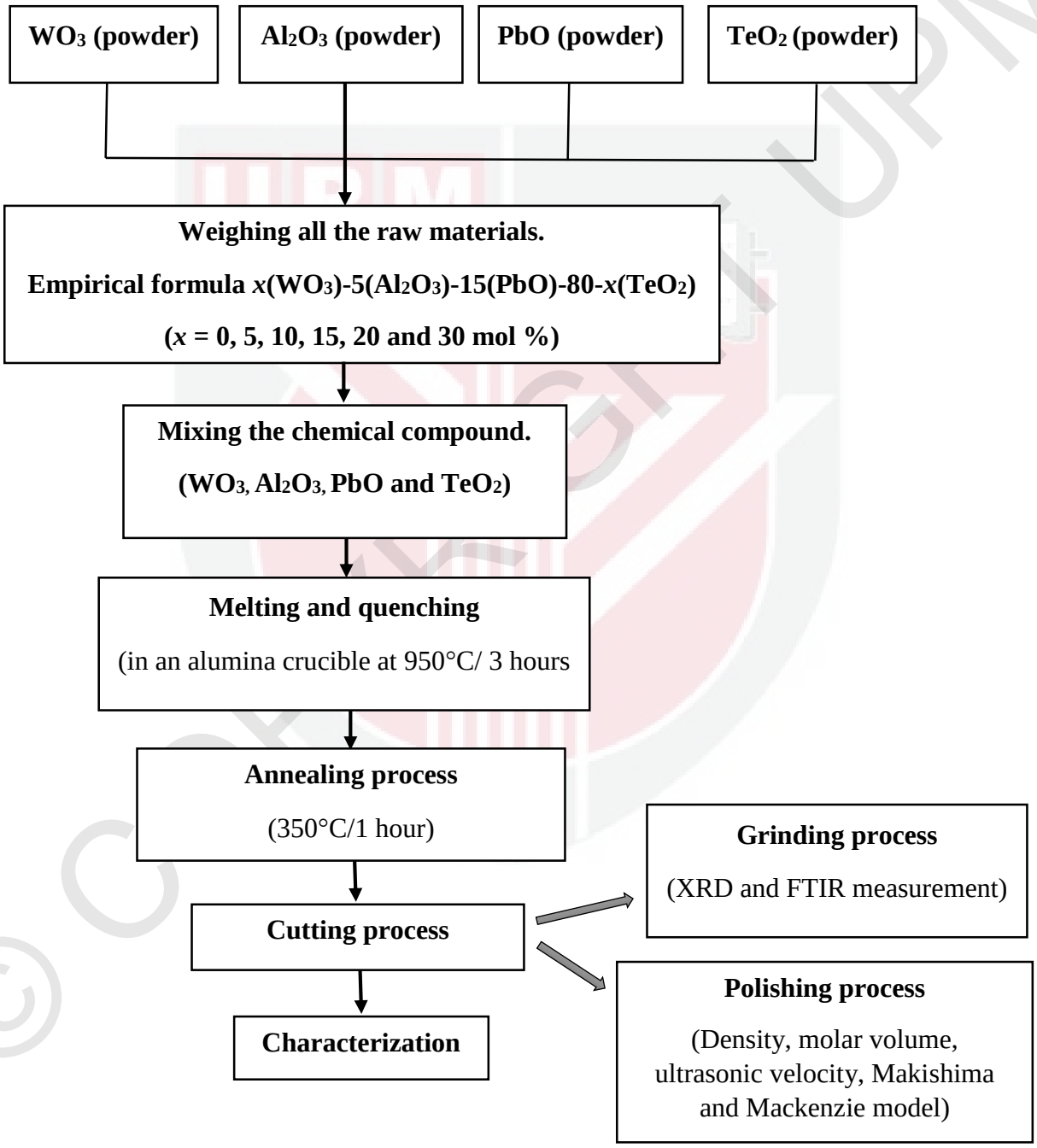

Figure 3.1 Schematic diagram of melt-quenched technique

3.3 X-ray diffraction (XRD) Measurement

XRD is defined as a methodology for analysing and identifying the structure of glass samples (in powder form), regardless of whether the materials were crystalline or amorphous. It contains information on structures, phases, preferred crystal orientations (texture), and other structural factors like as grain size, crystallinity, strain, and crystal defects (Vishwakarma et al., 2020). The glass samples were analysed in powder form in this investigation, and the XRD results were produced in the form of a diffractogram. Additionally, the methodology may be used to provide quantitative data, such as estimating the number of various phases contained in a sample (Saini & Kaur, 2021). The technique's restriction is typically related to the penetration depth of X-rays into the substance being studied. Although the small penetration depth of metals limits this characterisation approach to surface layers, the weak diffraction pattern produced for thin coatings occasionally impairs the speed and accuracy of the study. Crystalline substances may react to X-ray wavelengths as three-dimensional diffraction gratings with spacings identical to those seen in a crystal lattice. X-ray diffraction is fundamentally based on the constructive interference of monochromatic X-rays with a crystalline sample distributed by ordered features. The cathode rays create the X-rays in various kinds of glass tubes, producing monochromatic radiation that is aimed at the sample from a range of angles. The lattice should be created due to the random orientation of the powdered material with combinations of possible diffraction directions while scanning the sample throughout a range of two theta angles.

The constructive interference, or Bragg peaks, are formed as a result of the incident rays interacting with the samples. It met the requirements of Bragg's Law. This rule establishes a relationship between the wavelength of electromagnetic radiation and the diffraction angle and lattice spacing of a crystal. Bragg's law established the crystal structure and revealed the precise locations of atoms. The intensity fluctuation reflected from the beam will be converted to a graph (intensity vs. angle). The Bragg's law relationship:

$$n\lambda = 2d\sin\theta \tag{3.1}$$

where n is an integer, d is the inter-planar distance between the atomic lattice planes, is the X-ray wavelength, and is the diffraction angle between the incoming beam and the scattering planes. Calculations, observations, and processing of the diffracted X-rays will next be performed. However, the primary objective of utilising Bragg's rule is to determine the angle of constructive interference created when X-rays bombard a parallel plane of atoms, resulting in the diffraction peak. Additionally, the d-spacing of a crystal is employed for identification and categorization purposes. Inter-planar spacing is the distance between the crystal lattice planes of atoms that cause constructive interference (d-spacing). The illustrations of the process diffracted X-rays beam on a fixed crystal plane at an angle are shown in Figure 3.2.

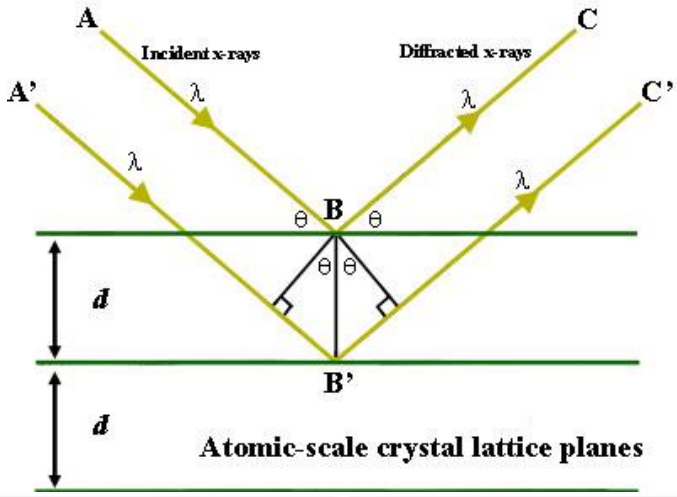

Figure 3.2 Bragg's Law reflection. The diffracted X-rays exhibit constructive interference when the distance between paths ABC and A'B'C' differs by an integer number of wavelengths (λ) (Henry & Mogk, 2016).

3.4 Density

The volume v associated with an oxygen ion has been computed in A^3 or 10^{-24} cm^3 units using the chemical composition and density of several hundred glasses (States et al., 1958). WO_3 functions as a network of intermediates or modifiers in glass based systems. The density of glass can be demonstrated as:

$$\rho_{glass} = \left(\frac{w_a}{w_a - w_w} \right) \rho_w \qquad (3.2)$$

Where w_a and w_w is the samples of glass weight in air and in water, respectively and ρ_w is the density of water.

The adding of WO_3 material increases the density of the tested glasses while decreasing the volume of molars. The molar volume was defined as the volume occupied by a unit mass of glass, and it was significantly impacted by the ionic radii of the oxides included into the glass. The density increase may be explained by the additional WO_3 oxide having a higher molecular weight. Generally, density is determined using the fluid displacement technique, which is based on the Archimedes principle. The buoyancy matches the weight of the displaced fluid, according to Archimedes's principle. The density of the glass samples was determined using the Archimedes Principle and xylene as the buoyant medium. A digital balance was used to make all measurements (contech). If the sample interacts with water, an inert liquid such as xylene, toluene, or other appropriate inert liquids may be used as the immersion medium (Chanshetti et al., 2011).

3.5 Molar volume

The molecular weight of the glass was also determined as mentioned below, and the molar volume of the glass samples may be estimated using the following expression:

$$V_m = \Sigma \frac{x_i M_i}{\rho} \tag{3.3}$$

Here, V_m denotes the molar volume, is the sample's density, and M is the sample's molecular weight. The immersion fluid and density values presented here are the mean of at least three independently measured measurements (Chanshetti et al., 2011). In this analysis, the molar volume is displayed to diminish by increasing the mol percentage of WO_3.

The next formula has been used to calculate the oxygen molar volume (V_o):

$$Vo = V_m \left(\frac{1}{\sum x_i n_i}\right) \tag{3.4}$$

3.6 Ultrasonic velocity measurement

The ultrasonic velocity of the specimens was determined using an AZ Industry Supplier MG 2000S ultrasonic thickness metre (Warsaw, Poland). Fig. 1 depicts a schematic representation of the ultrasonic study. The device had a built-in timer and was controlled in time-of-flight mode using the through-transmission method. Two conventional (longitudinal wave) transducers with a frequency of 2 MHz were utilised to detect longitudinal velocity. The velocity readings were accurate to within 1 ms^{-1} (Wróbel et al., 2007).

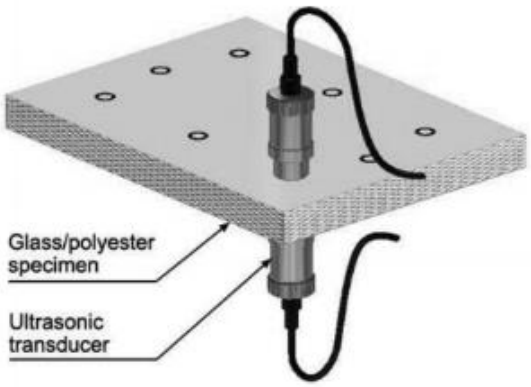

Fig 3.3 Scheme of the ultrasonic testing of wave velocity (Wróbel et al., 2007).

The ultrasonic wave velocity (c) was determined on the basis of well-known formula 3:

$c = h / \tau$, (3)

where h is the thickness of the specimen in the place where transducers

were put against it and τ is the time-of-flight of the ultrasonic wave.

Analysis of the ultrasonic velocity was obtained by evaluating via a pulse superposition method at room temperature, the time in between two simultaneous glass sample surfaces.

This pulse shows on the screen of a flaw detector when it is generated by a standard electrical circuit utilising the Ultrasonic Data Acquisition System (RITEC RAM-5000 S). Creating a NAP for the Probe model: With a resonance frequency of 5 MHz, the OLYMPUS A109S-RB generated a time pulse from a ceramic transducer and therefore functioned as a transmitter-receiver simultaneously. Ultrasonic velocity reactions can be determined by:

$$v = \frac{2d}{\Delta t} \tag{3.5}$$

Where d is the thickness of glass samples (cm) and is the time interval among the glass samples (s).

3.7 Elastic properties

Elasticity is defined as a material's capacity to deform when subjected to force and revert to its original shape when the force is removed. Typically, solids are stressed under three different kinds of conditions: uniaxial stress, triaxial stress, and pure shear (Nazrin et al., 2021). The ratio of each of these three stresses to the strain formed is Young's modulus, shear modulus, and bulk modulus respectively as illustrated in Fig. 1.

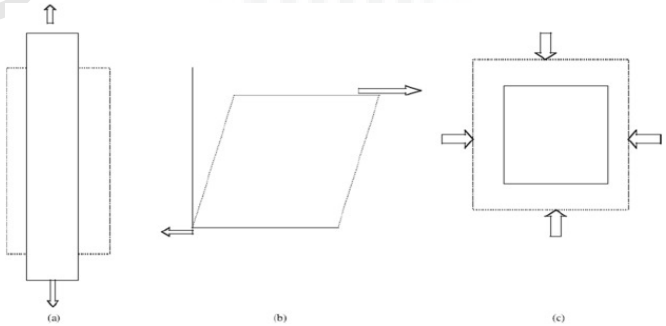

Fig 3.4 Illustration definition of constant of elasticity: a) Young's modulus; b) shear modulus; c) bulk modulus (Nazrin et al., 2021).

Additionally, the same parameter is used to determine the strength of a material when it is subjected to force. Elastic characteristics are also a critical factor to consider when choosing glass samples for a certain application. The two velocities are very important tools for the investigation of elastic properties of a glass material (Tafida et al., 2020). The values are calculated using the following relation.

$$V = \frac{2d}{\Delta t}$$

Where d represents the thickness of the sample, V is the ultrasonic wave velocity and Δt represents the time difference for the two measured times of flight respectively.

3.8 Makishima and Mackenzie model

The Makishima-Mackenzie (MM) model, developed theoretically, describes the Young's modulus of glass in terms of two deciding variables, namely the inter-atomic bonding strength (dissociation energy) and the arrangement of atoms (atomic packing fraction). While this straightforward model provides a clear physical image of the compositional dependence of the stiffness of glasses, it often underestimates the real Young's modulus for many glasses, particularly those with large values. As for suggestion in this research that the MM model's insufficiency stems mostly from its definition of the atomic packing fraction which is defined as the ratio of the atoms' volumes to the actual macroscopic volume of the glass (Shi et al., 2020).

$$E = 2V_t \sum_i G_i x_i$$

where E is the Young's modulus, Vt is the atomic packing fraction (the percentage of space filled with all kinds of ions), Gi is the dissociation energy of component I per unit volume, and

xi are the mole fractions. The glass's ingredients are believed to be the oxides, such as SiO2, Na2O, and CaO in a soda-lime-silicate glass. This model is often used to predict the stiffness of glass and to link results with composition. Indeed, it is discovered empirically that this model accurately describes silicate glasses to within approximately 20% (Plucinski & Zwanziger, 2015).

The Makishima and Mackenzie model was used to theoretically estimate both longitudinal and shear ultrasonic wave velocities for a variety of tellurite glasses. The model is mostly dependent on the values of the density obtained experimentally. Then, in this search work, the problems of determining the measured densities of amorphous glasses (because the density is dependent on the geometry of the network structure of these glasses) and the slope of linear regression between the experimentally determined bulk modulus and the product of packing density and experimental Young's modulus were solved. The findings indicated a high degree of consistency between empirically obtained densities and both ultrasonic wave velocities and theoretically predicted values (Gaafar, 1970).

3.10 Rocherulle Model

Rocherulle's model suggested a revision to Makishima and Mackenzie's theoretical model. The model considers the elastic characteristics of individual oxides when calculating the overall elastic properties of oxide glasses. Individual oxide densities and molecular masses were examined in place of the Makishima-Mackenzie model's bulk glass density and molecular weight (Umar & Ibrahim, 2020). Modified expression of the Makishima and Mackenzie model was proposed by Rocherulle et al. (1989). The packing density, V_i in the Makishima-Mackenzie model is replaced with Ci which is expressed as follows:

$C_i = N_A(\frac{4\pi\rho}{3M})(xR_A^3 + yR_0^3)$

For glasses of poly component nature, the factor Ct is therefore expressed as follows:

$C_t = \sum_i C_i x_i$

$C_t = \sum_i \frac{\rho_i}{M_i} V_i x_i$

The fundamental difference between the two models is that the Makishima and Mackenzie models take the bulk density and molecular weight of the glass into account, while the Rocherulle model takes the density and molecular weights of the individual oxides into account. The theoretical calculation of the elastic modulus of glass using Rocherulle's model indicates that the elastic modulus of glass is composition and dissociation energy dependent (Makishima and Mackenzie, 1973). The elastic modulus determined by this model is independent of the density of the sample glass but is dependent on the density of each oxide in the glass. The primary objective of this study is to compare the experimental values of elastic modulus acquired using the pulse echo technique to the theoretical values derived using the Rocherulle model (Zaid et al., 2011).

CHAPTER 4

RESULTS AND DISCUSSION

4.1 Introduction

This chapter examined the measurements for the glass samples' structural and elastic properties. The series of glasses with empirical formula $x(WO_3)$-5(Al_2O_3)-15(PbO)-80-$x(TeO_2)$ where x = 0, 5, 10, 15, and 20 mol % were prepared using the melt quenching technique. All the glass samples were transparent, homogeneous and bubble-free. Precursor glass was successfully prepared in a series. XRD, FTIR, ultrasonic velocities, density, molar volume, and structural and elastic model attributes were used to investigate the glass formation behaviour and structural and elastic characteristics. The acquired results and the glass characterization are presented.

4.2 Physical properties

4.2.1 Density and molar volume of glasses

Using a traditional melt and quenching procedure, a series of WO_3-Al_2O_3-PbO-TeO_2 pure powders were effectively melted and converted into a glass. Table 4.1 below shows the density (ρ) and molar volume (Vm) of glass samples. The density plays an important role and also an important physical property that capable to explain the changes in glasses composition. A plot of density and molar volume of WO_3-Al_2O_3-PbO-TeO_2 glass sample as shown in Figure 4.1. As shown in the figure, the density of the glasses is increases from 6.232 to 6.847 g/cm^3 with

the addition of WO_3 content. The increasing of the density of the network glass system is causing the changes in cross-link density (El-Adawy & Moustafa, 1999).

The density (ρ) and molar volume (V_m) for glass systems are opposite trend to each other and it shows that the Vm decrease with an increase of WO_3 content. The values of V_m decrease from 26.68 to 26.39 cm^3/mol and this is due to the WO_3 content that introduced in the network glass system.

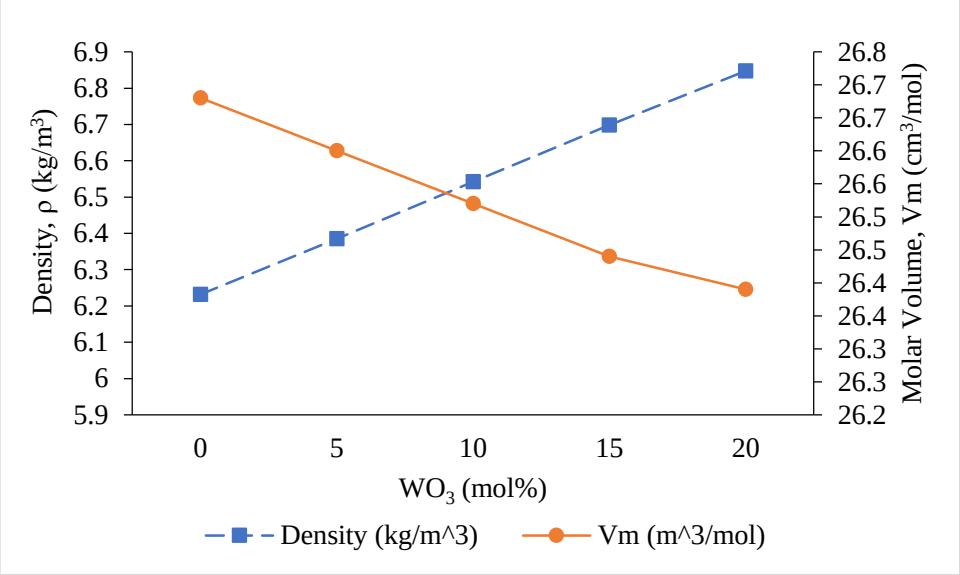

Figure 4.1 Density (ρ) and molar volume (V_m) of the WO_3-Al_2O_3-PbO-TeO_2 glass system.

Table 4.1: Density (ρ), molar volume (Vm), oxygen molar volume (V_o) and oxygen packing density (OPD) of the WO_3-Al_2O_3-PbO-TeO_2 glasses.

Glass sample	Molar percentage (mol%)			
	ρ (g/cm^3)	**Vm (cm^3/mol)**	**Vo (cm^3/mol)**	**OPD (mol/ L)**
G1	6.232	26.68	14.04	71.22
G2	6.385	26.60	13.64	73.30
G3	6.542	26.52	13.26	75.42
G4	6.698	26.44	12.90	77.53
G5	6.847	26.39	12.57	79.57

4.2.2 Oxygen molar volume and oxygen packing density

A plot of oxygen packing density (OPD) and oxygen molar volume (Vo) of WO_3-Al_2O_3-PbO-TeO_2 glass sample is shown in Figure 4.2. It shows that OPD and Vo for the network glass system are in opposite trend to each other. The values of OPD are increases from 71.22 to 79.57 mol/L while for Vo are decreases from 14.04 to 12.57 cm3/mol as the WO3 content are increase from 0 to 25 mol % for WO_3-Al_2O_3-PbO-TeO_2 glass system. This inverse trend in OPD and Vo could be attributed to the substitution of B2O3 with WO_3 as network glass systems get smaller and denser (Issa et al., 2019).

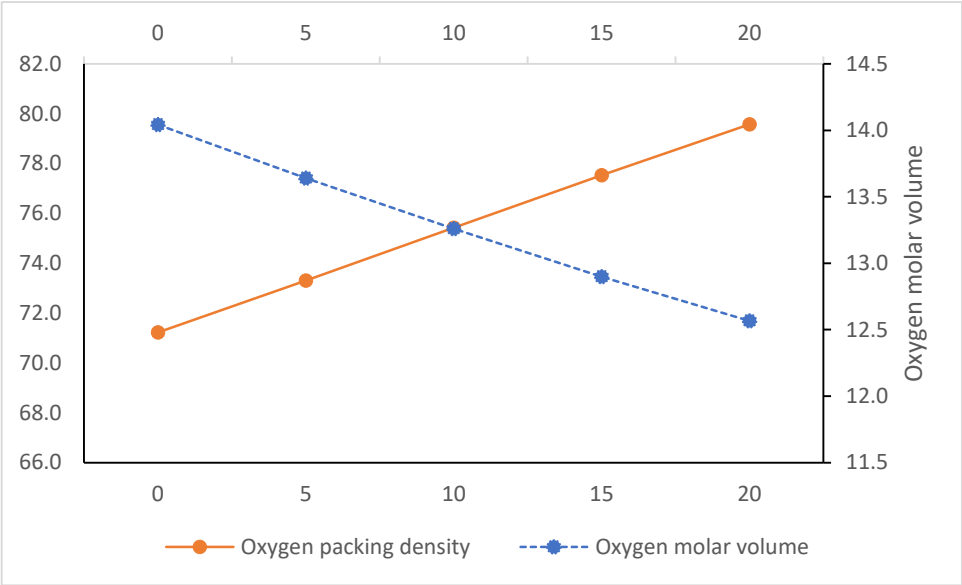

Figure 4.2 Oxygen packing density (OPD) and oxygen molar volume (V_o) of the WO_3-Al_2O_3-PbO-TeO_2 glass system.

4.3 Structural Properties

4.3.1 XRD Analysis

The XRD pattern of WO_3-Al_2O_3-PbO-TeO_2 is represents in Figure 4.3 with different amount of WO3 content. From figure 4.3, it is observed a broad halo peak at lower angle (below 40) with its maxima located at around $2\theta = 27°$ and no continuous sharp peak can be seen.

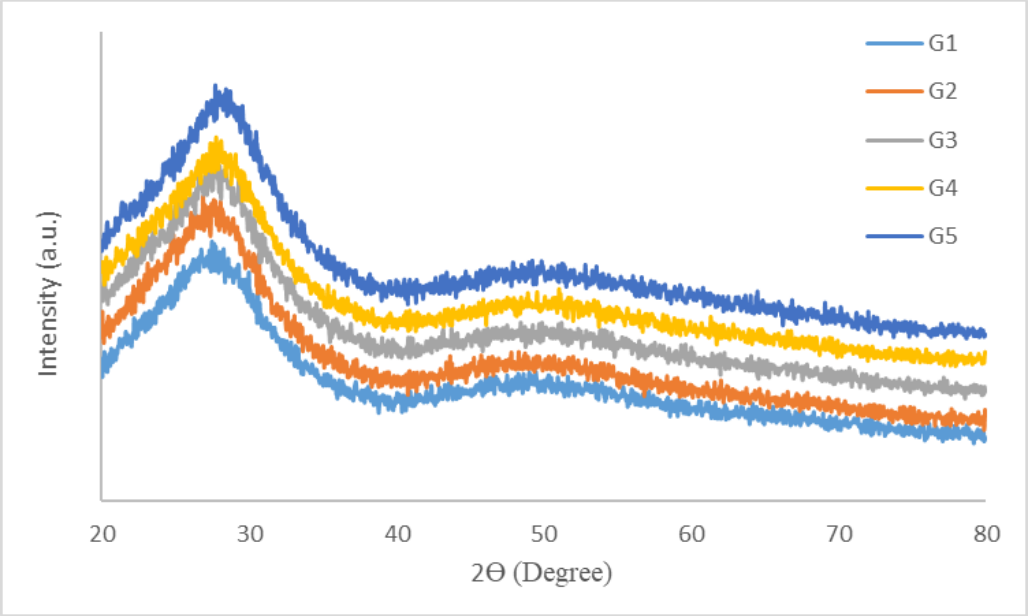

Figure 4.3 X-ray diffraction of WO_3-Al_2O_3-PbO-TeO_2 glass systems.

4.4 Elastic Properties

4.4.1 Ultrasonic Velocity

The studies of ultrasonic velocities play an important role to explain the changes in structural behavior of the network glasses composition. Figure 4.3 presents the longitudinal (V_L) and Shear (V_s) velocity variations for WO_3-Al_2O_3-PbO-TeO_2 glass systems with the increasing of WO_3 content. It seen that the longitudinal velocity (V_L) is increases from 2823 m/s (0 mol %) to 3289 m/s (20 mol %) while for shear velocity (V_s) is increases from 1600 m/s (0 mol %) to 1813 m/s (20 mol %) when the glass network is added with the WO_3 content.

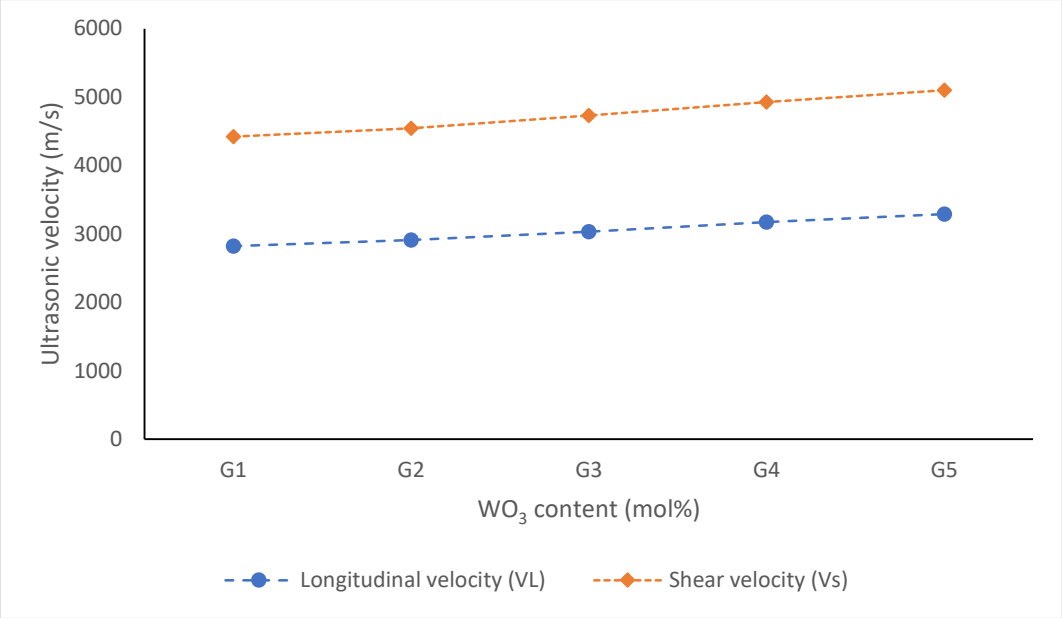

Figure 4.4 Variation change in longitudinal velocity (VL) and shear velocity (Vs) with respect to WO3 content for WO_3-Al_2O_3-PbO-TeO_2 at room temperature.

Table 4.2 The longitudinal (VL) and shear velocities (Vs) of the WO_3-Al_2O_3-PbO-TeO_2 glass systems.

Glass sample	WO3 (mol %)	VL (m/s)	Vs(m/s)
G1	0	2823	1600
G2	5	2911	1633
G3	10	3032	1698
G4	15	3171	1755
G5	20	3289	1813

4.4.2 Experimental elastic moduli

Table 4.3 displays the experimental values for longitudinal (L), shear (G), bulk (K), Young's (E) modulus, microhardness (H), and Poisson's ratio with the variation of mol percentage of WO3 content.

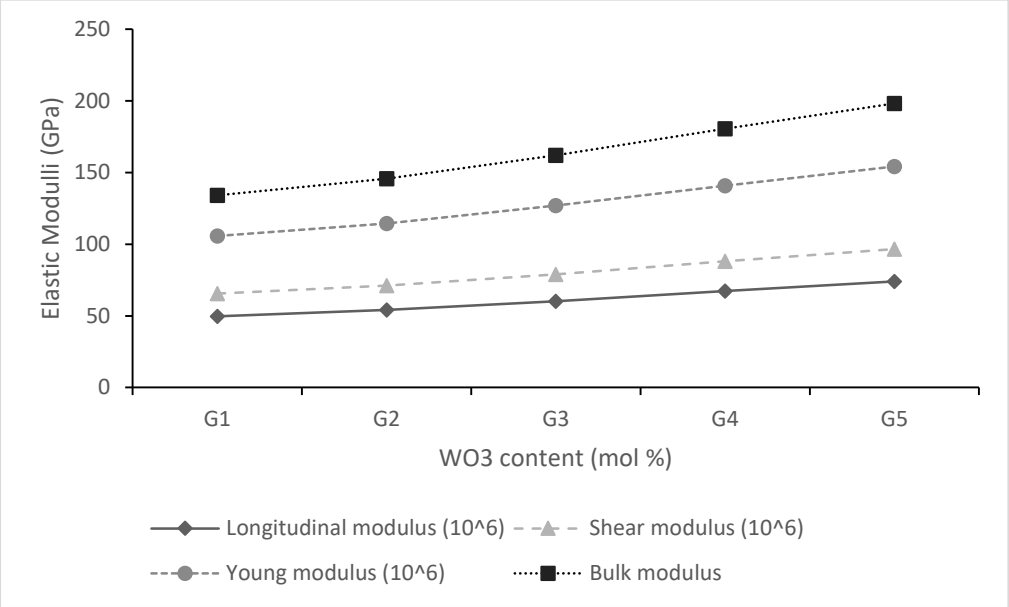

Figure 4.5 Elastic moduli longitudinal (L), shear (G), Young's (E) and bulk modulus (K) against the mol percentage of WO_3 for WO_3-Al_2O_3-PbO-TeO_2 glasses.

Table 4.3 Elastic properties result of longitudinal ultrasonic velocity (VL), shear ultrasonic velocity (Vs), longitudinal (L), shear (G), bulk (K), Young's (E) modulus, Microhardness (H) and Poisson's ratio (σ) of WO_3 for WO_3-Al_2O_3-PbO-TeO_2 glasses.

Glass Sample	VL (m/s)	Vs (m/s)	L (GPa)	G (GPa)	K (GPa)	H (GPa)	E (GPa)	σ
G1	2823	1600	49.66	15.95	28.39	2.51	40.19	0.263
G2	2911	1633	54.11	17.03	31.4	2.61	43.26	0.270
G3	3032	1698	60.14	18.86	34.99	2.86	47.9	0.272
G4	3171	1755	67.35	20.63	39.84	3.04	52.81	0.279
G5	1813	1813	74.07	22.51	44.06	3.27	57.63	0.282

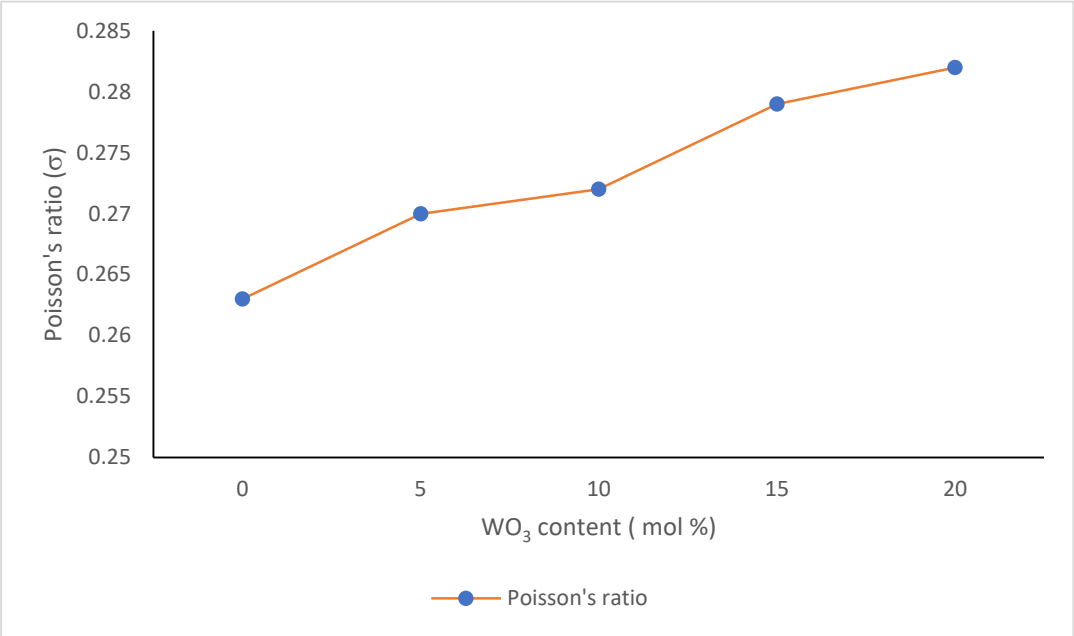

Figure 4.6 Poisson's ratio (σ) with respect to WO_3 content for WO_3-Al_2O_3-PbO-TeO_2 at room temperature.

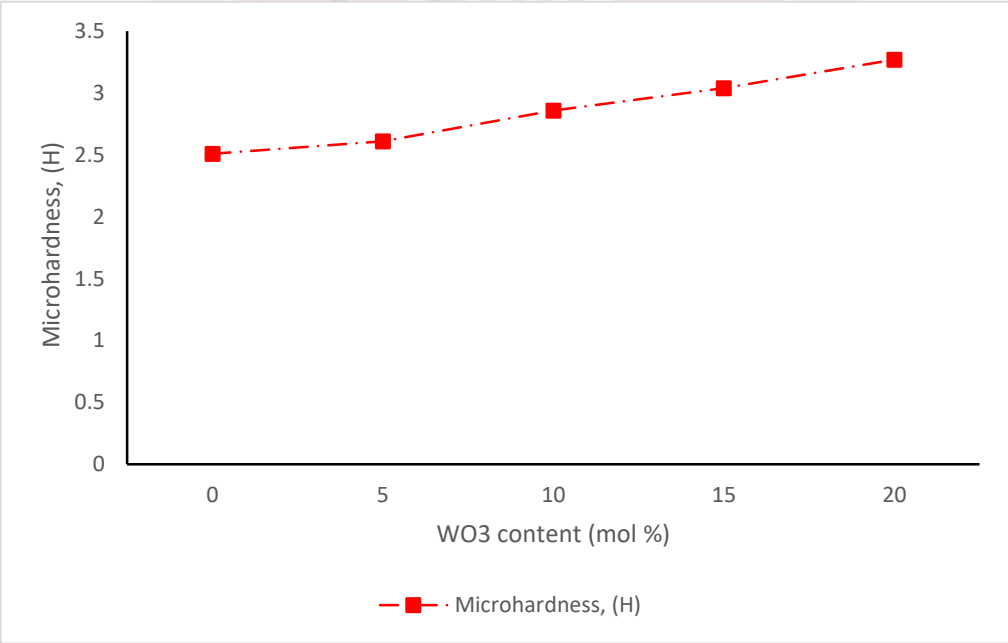

Figure 4.7 Microhardness (H) with respect to WO_3 content for WO_3-Al_2O_3-PbO-TeO_2 glass system at room temperature.

4.4.3 Rocherulle model

Rocherulle theoretical model is an extension of Makishima and Mackenzie's theory and Rocherulle theoretical model suggested that the packing factor and dissociation energy in the glass composition affected the value of elastic moduli (Rocherulle *et al.,* 1989).

Table 4.4 displays the theoretical elastic moduli that been calculated by using Rocherulle model. All elastic moduli which is longitudinal, shear and Young's modulus are found to be increase when content of WO_3. . The increasing in longitudinal modulus from 34.01 to 36.83 GPa, shear modulus from 9.95 to 11.32 GPa, and Young's modulus from 20.26 to 23.94 GPa while the increasing of bulk modulus from 13.21 to 14.76 has been observed. For microhardness and Poisson's ratio both are increasing which microhardness from 1.04 to 2.12 and poisson's ration from 0.284 to 0.410 with the increments of WO_3 content.

Table 4.4 Elastic properties result of longitudinal (L), shear (G), bulk (K), Young's (E) modulus, Hardness (H) and Poisson's ratio (σ) of WO_3-Al_2O_3-PbO-TeO_2 glasses using Rocherulle model.

Glass sample	L_R (GPa)	G_R (GPa)	K_R (GPa)	E_R (GPa)	H_R (GPa)	σ_R
G1	34.01	9.95	13.21	20.26	1.04	0.284
G2	34.92	10.23	13.89	21.33	1.24	0.354
G3	35.61	10.68	14.06	22.05	1.53	0.360
G4	36.15	10.92	14.45	23.16	1.89	0.366
G5	36.83	11.32	14.76	23.94	2.12	0.410

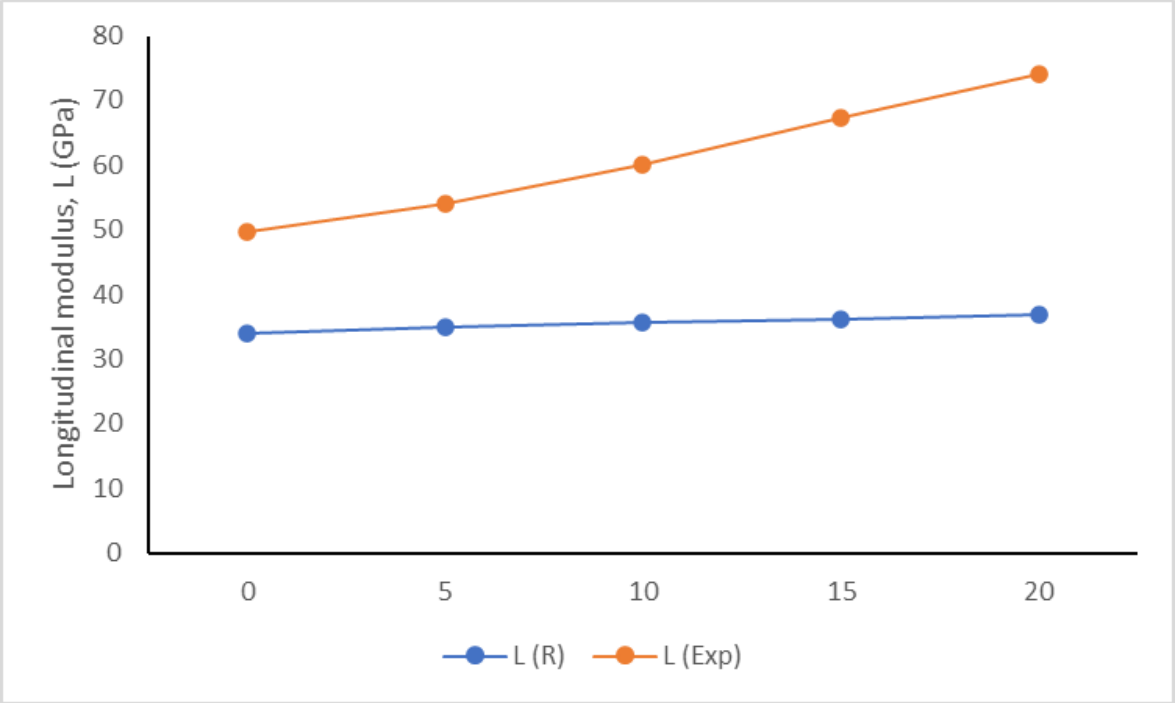

Figure 4.8 Agreement between the experimental values of Longitudinal modulus and that calculated using Rocherulle model for WO_3-Al_2O_3-PbO-TeO_2 glass system.

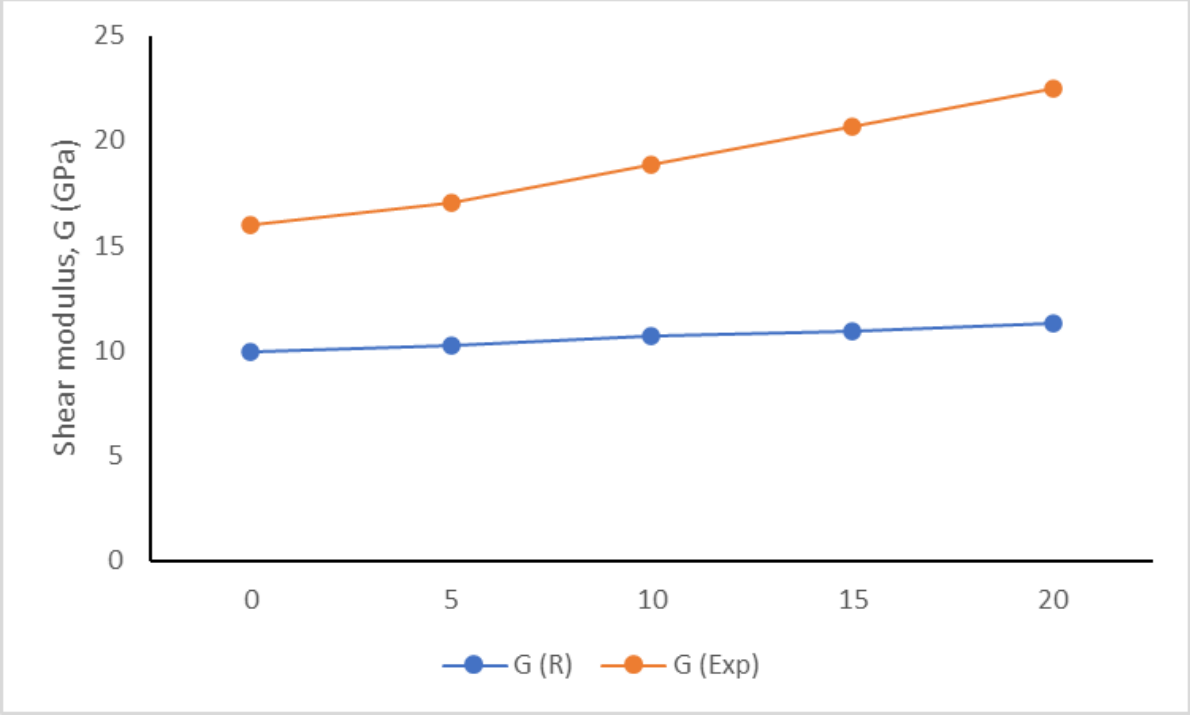

Figure 4.9 Agreement between the experimental values of Shear modulus and that calculated using Rocherulle model for WO_3-Al_2O_3-PbO-TeO_2 glass system.

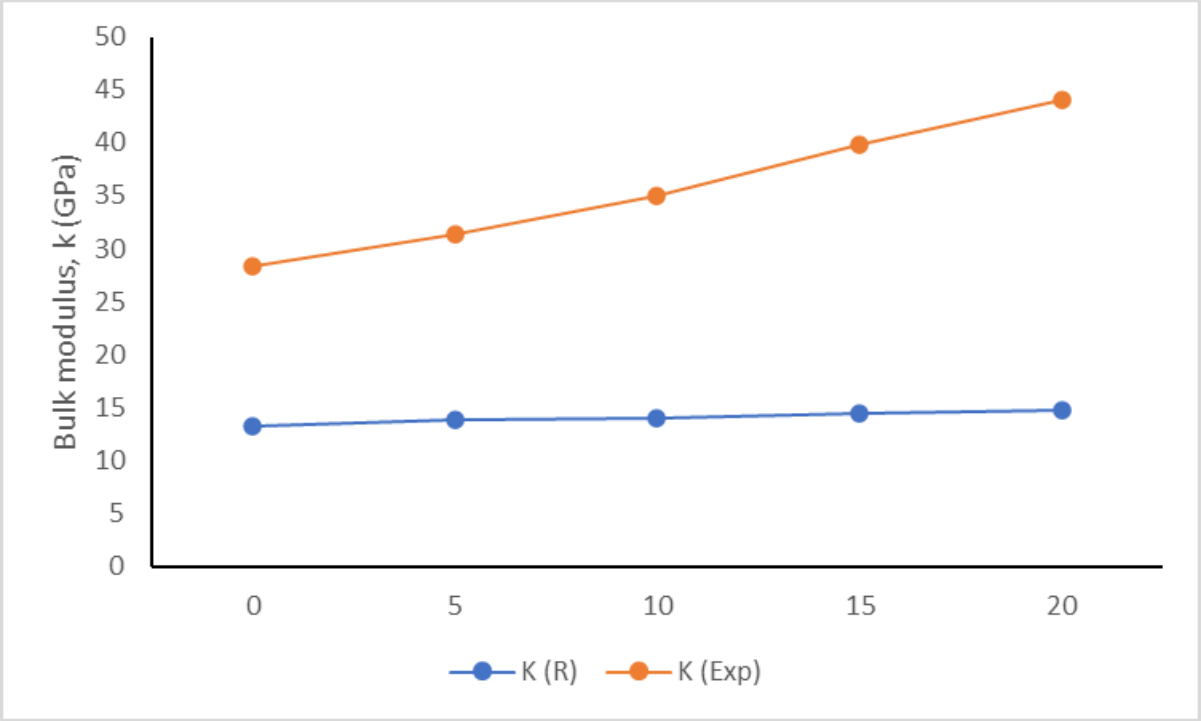

Figure 4.10 Agreement between the experimental values of Bulk modulus and that calculated using Rocherulle model for WO_3-Al_2O_3-PbO-TeO_2 glass system.

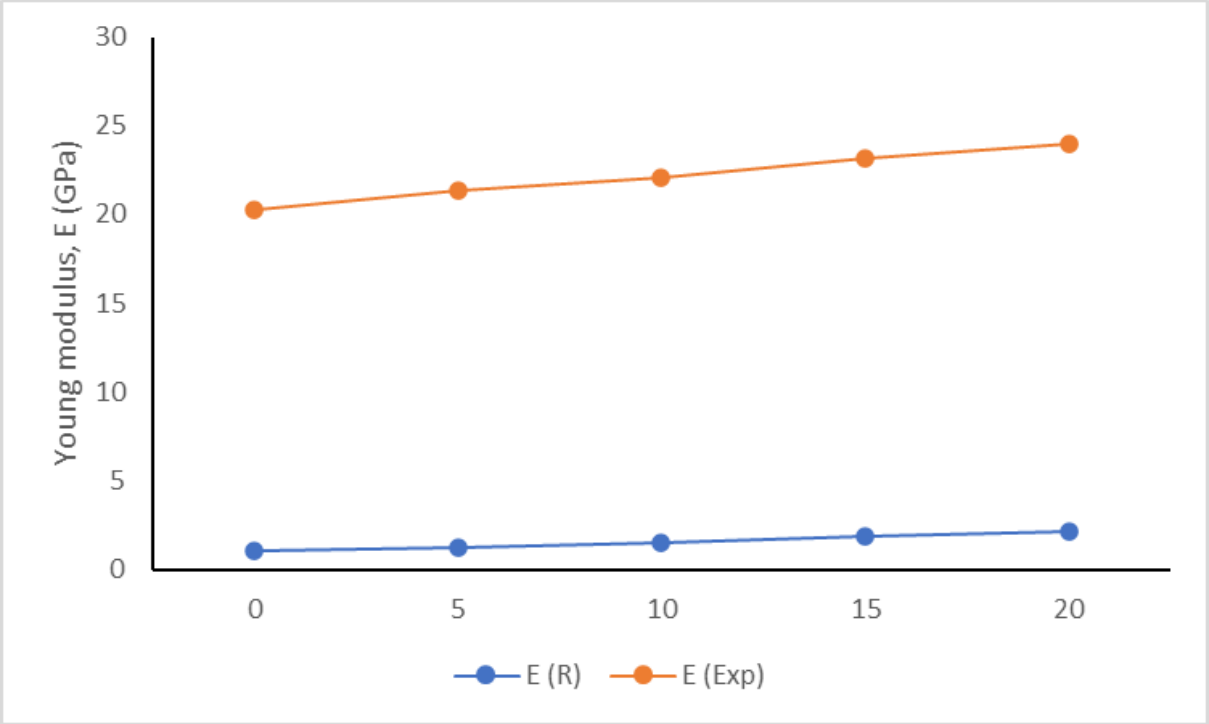

Figure 4.11 Agreement between the experimental values of Young's modulus and that calculated using Rocherulle model for WO_3-Al_2O_3-PbO-TeO_2 glass system.

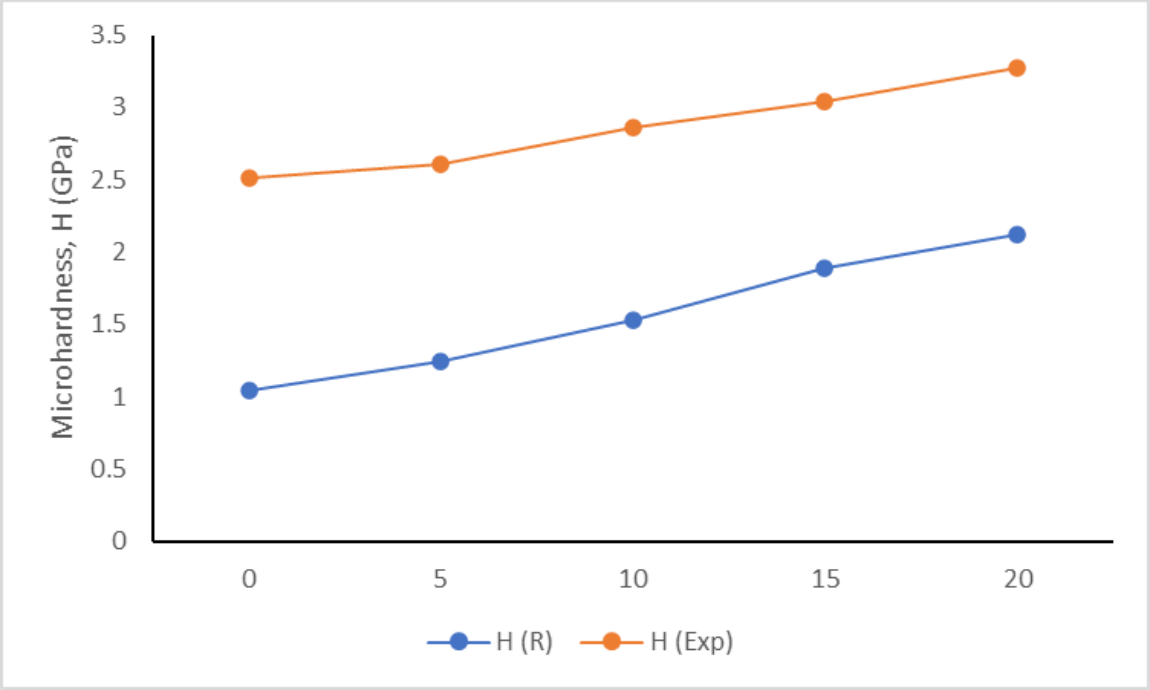

Figure 4.12 Agreement between the experimental values of Microhardness and that calculated using Rocherulle model for WO_3-Al_2O_3-PbO-TeO_2 glass system.

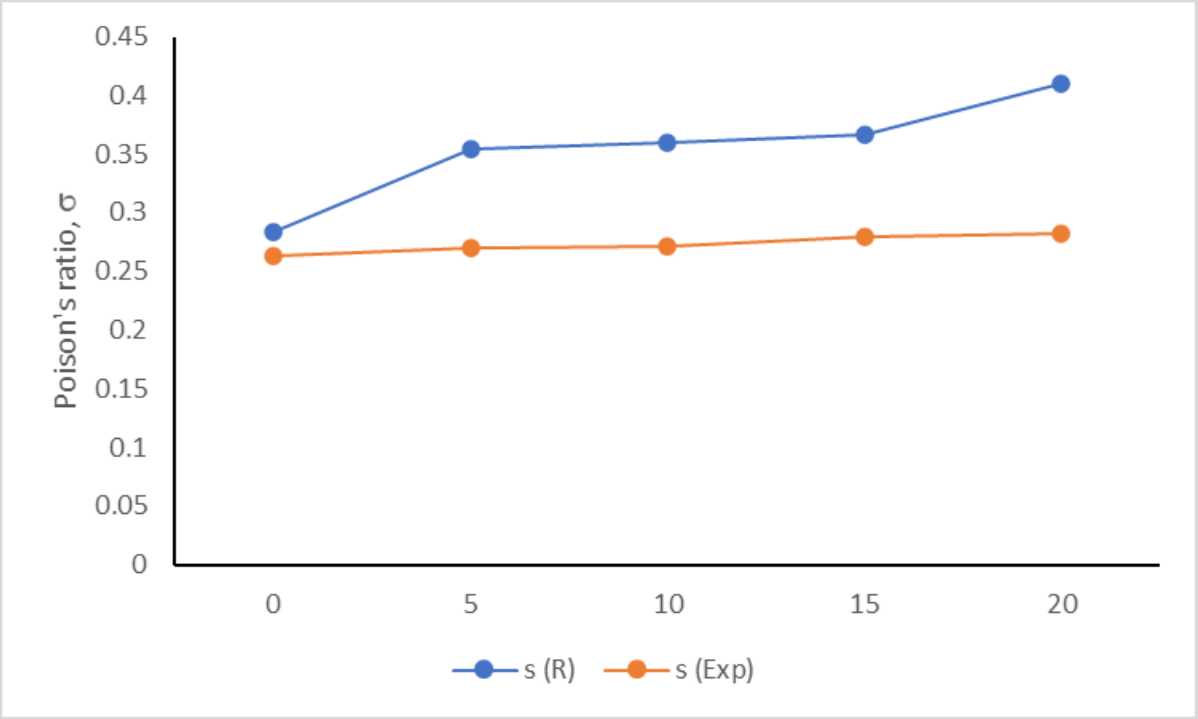

Figure 4.13 Agreement between the experimental values of Poisson's ratio and that calculated using Rocherulle model for WO_3-Al_2O_3-PbO-TeO_2 glass system.

4.4.4 Makishima and Mackenzie model

The elastic moduli that had been calculated by using Makishima and Mackenzie model were considered the dissociation energy per unit volume (G_t) and packing density (V_t) of oxides in glass composition (El-Moneim, 2016; Effendy *et al.*, 2020).

According to the Makishima and Mackenzie model, the theoretical values of elastic moduli, microhardness (H) and Poisson's ratio are listed in **Table 4.5**. As been observed in **Table 4.5**, the theoretical values of elastic moduli are increase with increasing WO_3 content. The addition of WO_3 content to the glass system caused the longitudinal modulus to increase from 25.27 to 27.31 GPa, shear modulus increases from 8.75 to 9.88 GPa, Bulk modulus increases from 10.67 to 12.06 GPa and Young's modulus increase from 23.15to 27.15 GPa.

Fig. 4.14 until **Fig. 4.17** illustrated the comparison between experimental and theoretical elastic moduli (Makishima and Mackenzie model) while **Fig. 4.18** and **Fig. 4.19** illustrated the comparison between experimental microhardness and experimental Poisson's ratio with theoretical values respectively with an increasing WO_3 concentration. The correlation percentage between theoretical and experimental values for longitudinal modulus ranges between 99.93 percent and 99.21 percent, for shear modulus between 99.99 percent and 99.58 percent, for bulk modulus between 99.53 percent and 98.31 percent, and for Young's modulus between 99.96 percent and 99.53 percent, as shown in these figures. The correlation percentage between theoretical and experimental values for microhardness and Poisson's ratio, on the other hand, ranges between 99.99 percent and 99.36 percent for microhardness and 99.95 percent and 89.81 percent for Poisson's ratio, respectively. These findings imply that the Makishima

and Mackenzie model is better suitable for forecasting elastic moduli, microhardness, and Poisson's ratio for WO_3-Al_2O_3-PbO-TeO_2 glasses than the Rocherulle model. It is believed that the Makishima and Mackenzie model is valid for all investigated glass samples and gives excellent agreement between the calculated and observed values of the elastic moduli, microhardness, and Poisson's ratio due to the effect of the structural units present in the network glass system.

Table 4.5 Elastic properties result of longitudinal (L), shear (G), bulk (K), Young's (E) modulus, Hardness (H) and Poisson's ratio (σ) of WO_3-Al_2O_3-PbO-TeO_2 glasses using Makishima and Mackenzie model.

Glass Sample	L_{MM} (GPa)	G_{MM} (GPa)	K_{MM} (GPa)	H_{MM} (GPa)	σ_{MM}	EMM (GPa)
G1	25.27	8.75	10.67	1.18	0.219	23.15
G2	25.78	8.92	10.93	1.37	0.225	23.68
G3	26.15	9.11	11.31	2.35	0.234	24.72
G4	26.96	9.63	11.72	2.78	0.239	26.56
G5	27.31	9.88	12.06	3.11	0.247	26.54

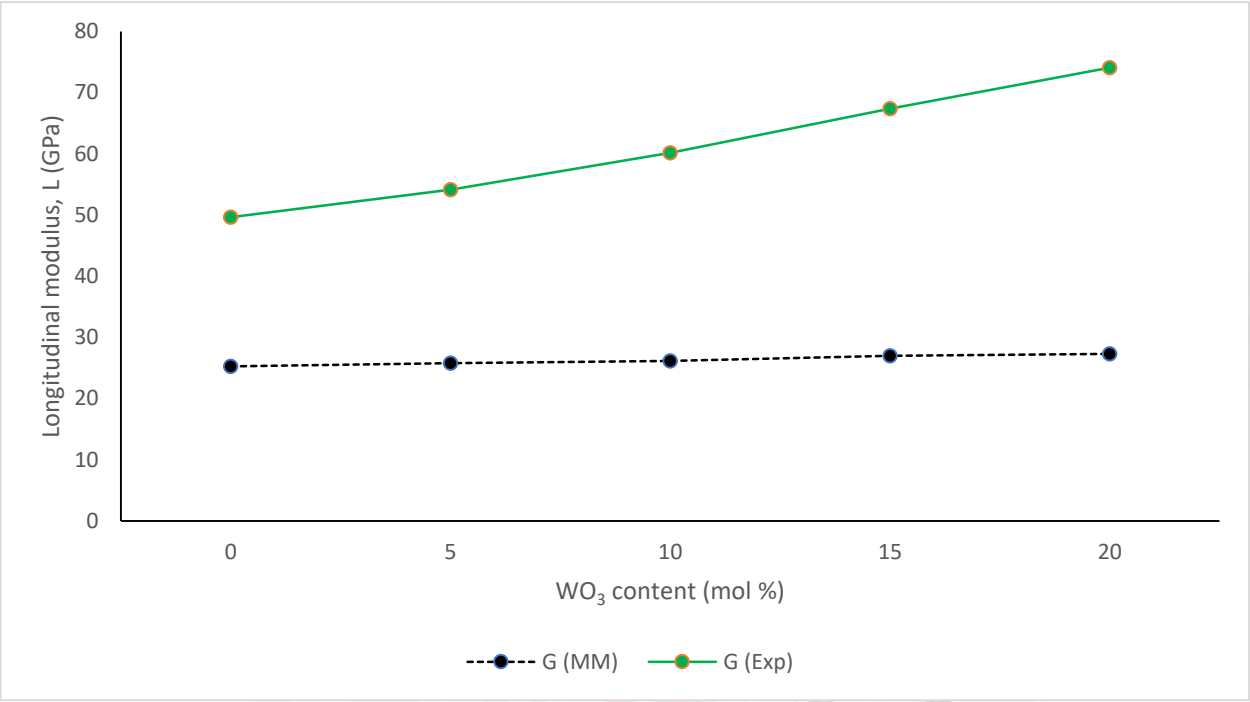

Figure 4.14 Longitudinal modulus from experimental and Makishima and Mackenzie's model prediction of WO_3-Al_2O_3-PbO-TeO_2 glass composition.

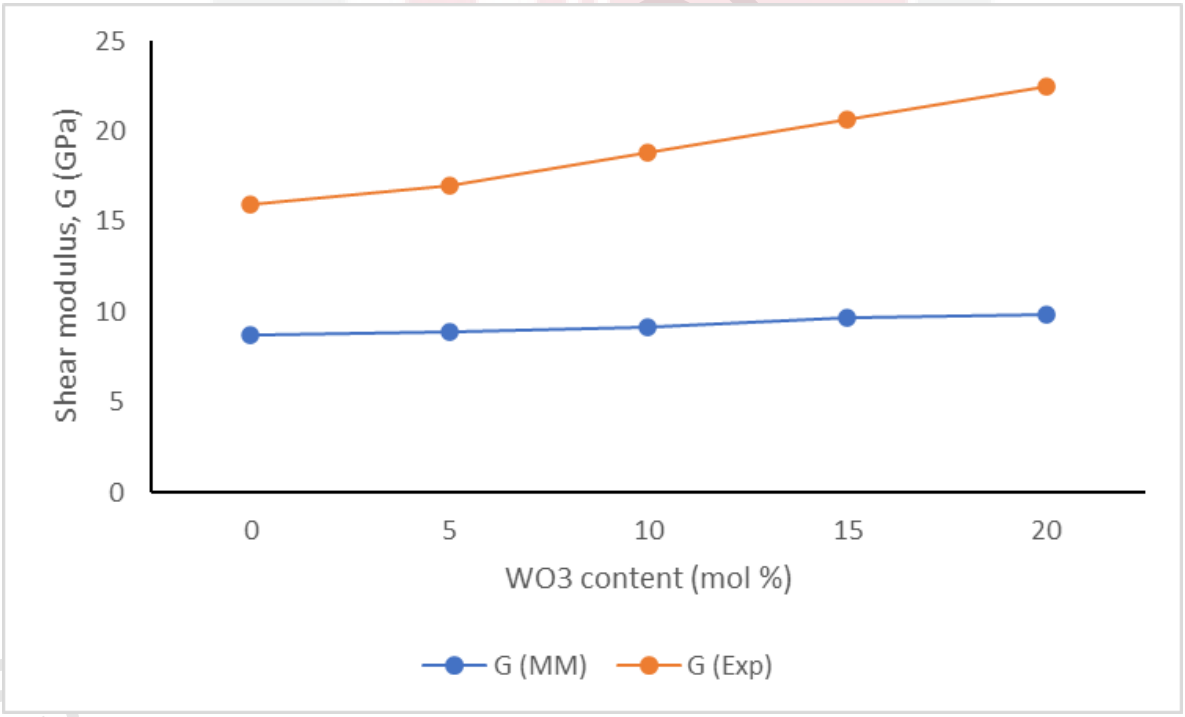

Figure 4.15 Shear modulus from experimental and Makishima and Mackenzie's model prediction of WO_3-Al_2O_3-PbO-TeO_2 glass composition.

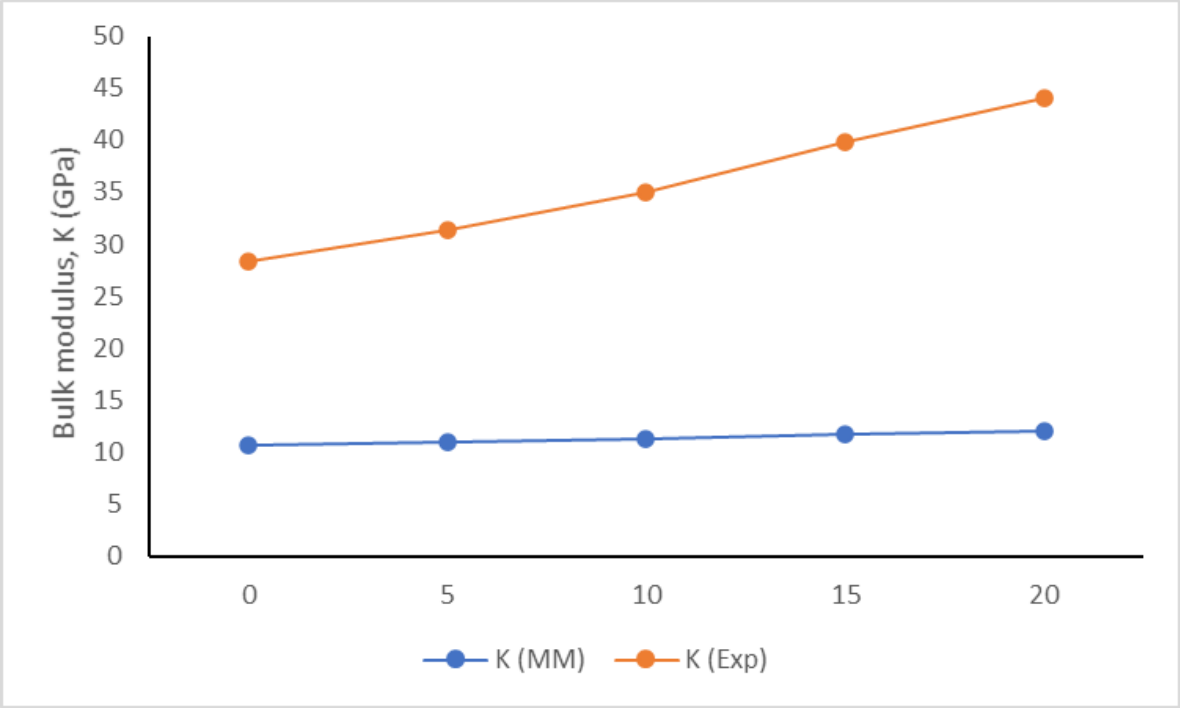

Figure 4.16 Bulk modulus from experimental and Makishima and Mackenzie's model prediction of WO_3-Al_2O_3-PbO-TeO_2 glass composition with WO_3 mol content $0 < x < 20$ mol %.

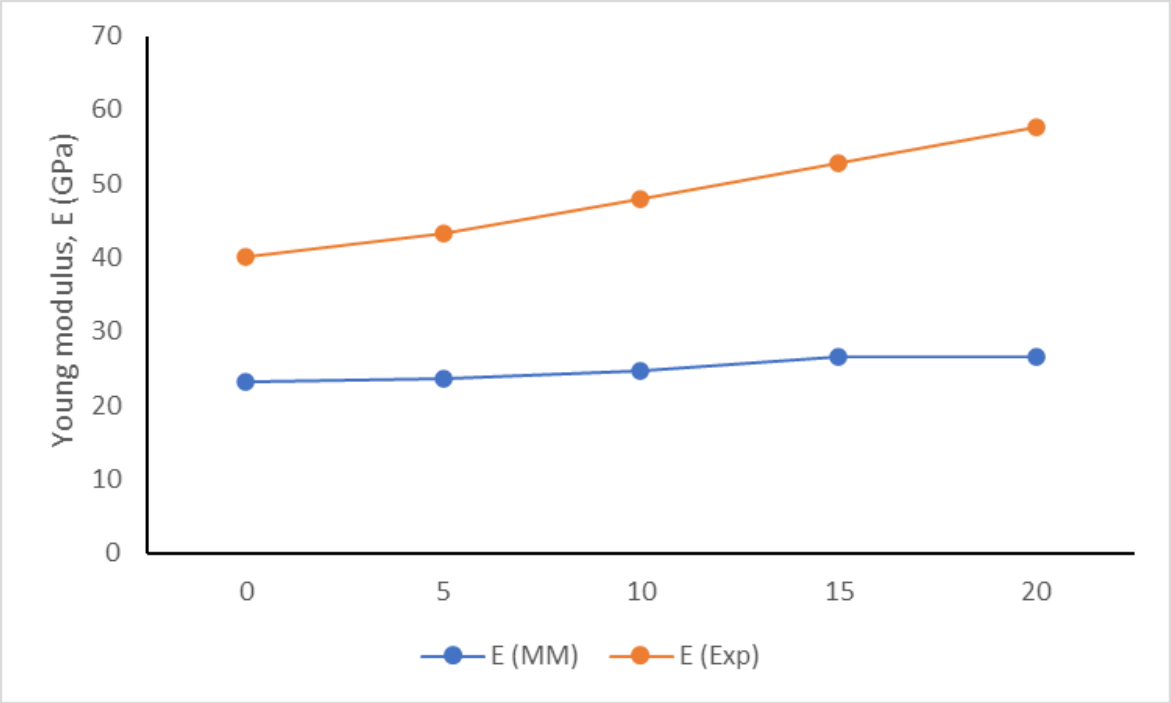

Figure 4.17 Young's modulus from experimental and Makishima and Mackenzie's model prediction of WO_3-Al_2O_3-PbO-TeO_2 glass composition.

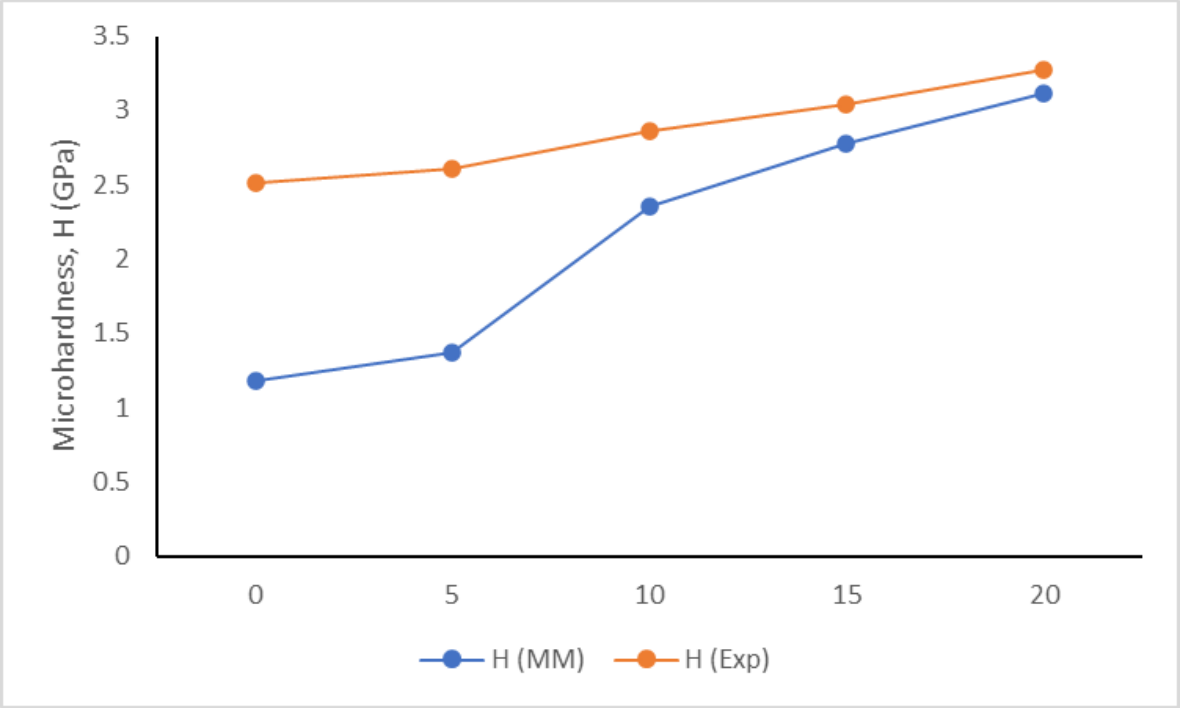

Figure 4.18 Microhardness from experimental and Makishima and Mackenzie's model prediction of WO_3-Al_2O_3-PbO-TeO_2 glass composition.

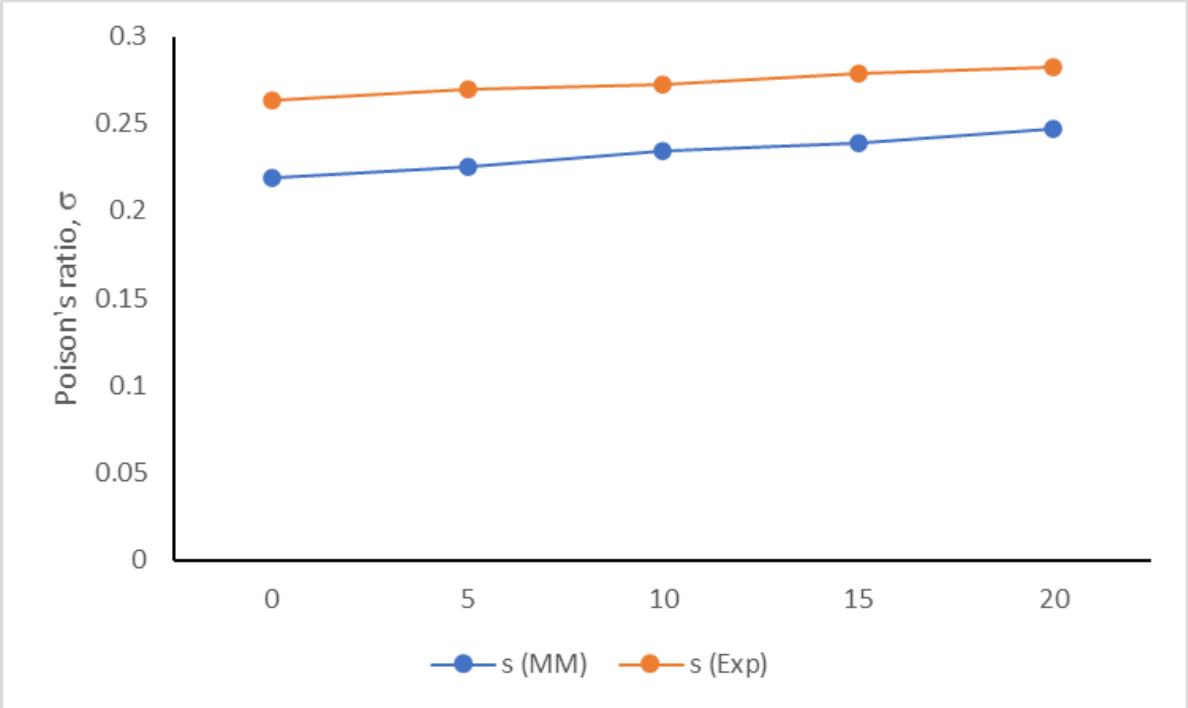

Figure 4.19 Poisson's ratio from experimental and Makishima and Mackenzie's model prediction of WO_3-Al_2O_3-PbO-TeO_2 glass composition.

CHAPTER 5

CONCLUSION DAN RECOMMENDATIONS

5.1 Introduction

The primary purposes of this study were to analyses the structural and elastic properties of WO_3-Al_2O_3-PbO-TeO_2 glass system by a quenching technique that is used in various fields. In order to understand the properties of the network glass system, all precursor glass was prepared with the approximate compositions and analysed using Archimedes method, XRD, ultrasonic velocities, experimental elastic moduli and theoretical elastic moduli (Makishima and Mackenzie model and Rocherulle model). Observations of the results obtained throughout the process of the experimental and theoretical works leads to as the following conclusion.

5.2 Conclusion

In this studies, the structural and elastic properties of WO_3-Al_2O_3-PbO-TeO_2 with x = 0, 5, 10, 15 and 20 mol % are demonstrated. Based on the result obtained, the density and molar volume of the precursor glass sample both were increased and decreased respectively with the increasing of WO_3 concentration. The increasing of oxygen packing density and the decreasing of oxygen molar volume advocates that the precursor glasses become more compact and denser. The physical and structural features of the glasses were determined

using density and molar volume measurements, as well as other characteristics such as XRD. A non-destructive ultrasonic spectroscopy was used to examine the elastic characteristics of the novel glass system. The elastic characteristics of the glass systems were determined using theoretical elastic models such as the Makishima-Mackenzie and Rocherulle model. The longitudinal and shear ultrasonic velocity both increasing with the rising of WO_3 concentration, which is produced by the production of more non-bridging oxygens in the network glass system as according to the ultrasonic velocities measurements. The experimental and theoretical elastic moduli (Makishima and Mackenzie model and Rocherulle model), as well the microhardness of the precursor glasses are all increased, while the Poisson's ratio of the precursor glasses decreased that indicates the glass system's rigidity is rising. Therefore, the WO_3-Al_2O_3-PbO-TeO_2 glasses appears to be promising for use in the field of optoelectronics as a potential optical amplifier.

5.3 Recommendations for future research

The current research was successfully studied on physical, structural, and elastic properties of WO_3-Al_2O_3-PbO-TeO_2 glasses via melting and quenching technique. However, there are a few ways to improve for further research.

1. Further study by using different kind of preparation methods for examples sol-gel, flux, solid state, and supercritical water method.
2. Research into various properties of WO_3-Al_2O_3-PbO-TeO_2 glasses, such as optical, thermal, electrical and dielectric properties.
3. Deeply study glasses with various qualities, such as phosphate and other glass systems.

4. Transition metals such as Lithium (Li+), sodium (Na+) and zinc (Zn2+) can all be applied as glass modifiers.
5. Include rare-earth dopants like europium, neodymium, and yttrium which can be used to improve the glass composition in optical devices.

Reference

Abd El-Moneim, A. (2019). Analysis and prediction of elastic moduli and Poisson's ratio in Li2O–B2O3–V2O5 glasses under the substitution of V2O5 for B2O3. Physics and Chemistry of Glasses: European Journal of Glass Science and Technology Part B, 60(4), 146–156.

Alazoumi, S. H. A. (2018, August 1). Elastic, optical and thermal properties of zinc-lead tellurite glass systems. Universiti Putra Malaysia Institutional Repository.

Bragg, W. (2002). The Glassy State. Structural Chemistry of Glasses, 13–76.

Chanshetti, U. B., Shelke, V. A., Jadhav, S. M., Shankarwar, S. G., Chondhekar, T. K., Shankarwar, A. G., Sudarsan, V., & Jogad, M. S. (2011). Density and molar volume studies of phosphate glasses. Facta Universitatis - Series: Physics, Chemistry and Technology, 9(1), 29–36.

El-Mallawany, R. (1998). Tellurite glasses Part 1. Elastic properties. Materials Chemistry and Physics, 53(2), 93–120.

Fares, H., Jlassi, I., Elhouichet, H., & Férid, M. (2014). Investigations of thermal, structural and optical properties of tellurite glass with WO3 adding. Journal of Non-Crystalline Solids, 396-397, 1–7.

Gaafar, M. S. (1970). Determination of Ultrasonic Velocities Theoretically for Tellurite Glasses Using Makishima and Mackenzie Model -. Journal of Engineering, Computing and Applied Sciences.

Ganzoury, M. A., & Allam, N. K. (2015). Impact of nanotechnology on biogas production: A mini-review. Renewable and Sustainable Energy Reviews, 50, 1392–1404.

Glass. Glass | School of Materials Science and Engineering. (n.d.). Retrieved from https://www.materials.unsw.edu.au/study-us/high-school-students-and-teachers/online-tutorials/ceramics/glass.

Grayson, K. (2020, February 8). Glass 101: Glass Formers – The Backbone of Glass. Mo-Sci Blog.

Grayson, K. (2020, February 8). Glass 101: Using Glass Modifiers to Change Glass Characteristics. Mo-Sci Blog.

Hauke, B., Barney, E. R., Crego, A., Tarantino, G., Affatigato, M., & Feller, S. (2018). Properties and Structure of Glassy TeO2 and Binary Potassium and Boron Tellurites. Journal of Undergraduate Reports in Physics, 28(1), 100001.

Hauke, B., Barney, E. R., Pakhomenko, E., Jesuit, M., Packard, M., Crego, A., Tarantino, G., Affatigato, M., & Feller, S. (2020). Structure and glass transition temperatures of tellurite glasses. *Physics and Chemistry of Glasses: European Journal of Glass Science and Technology Part B*, *61*(1), 21–26.

Helmenstine, Anne Marie, Ph.D. (2020, August 28). Glass Definition in Science. Retrieved from https://www.thoughtco.com/definition-of-glass-604484

Henry, D., & Mogk, D. (2016, November 10). *BraggsLaw*. Geochemical Instrumentation and Analysis. https://serc.carleton.edu/research_education/geochemsheets/BraggsLaw.html.

How an FTIR Spectrometer Operates. (2020, December 4). Retrieved June 15, 2021, from https://chem.libretexts.org/@go/page/1844

Issa, S. A. M., Susoy, G., Ali, A. M., Tekin, H. O., Saddeek, Y. B., Al-Hajry, A., Algarni, H., Anjana, P. S., & Agar, O. (2019, November 26). The effective role of LA2O3 contribution on zinc borate glasses: Radiation shielding and mechanical properties - applied physics a. SpringerLink. Retrieved February 11, 2022, from https://link.springer.com/article/10.1007/s00339-019-3169-5

Jaccani, S. P., Sundararaman, S., & Huang, L. (2018). Understanding the structural origin of intermediate glasses. Journal of the American Ceramic Society, 102(3), 1137–1149.

Mustafa, I., Kamari, H., Yusoff, W., Aziz, S., & Rahman, A. (2013). Structural and Optical Properties of Lead-Boro-Tellurrite Glasses Induced by Gamma-Ray. International Journal of Molecular Sciences, 14(2), 3201–3214.

Nazrin, S. N., Halimah, M. K., Muhammad, F. D., Latif, A. A., Iskandar, S. M., & Asyikin, A. S. (2021). Experimental and theoretical models of elastic properties of erbium-doped zinc tellurite glass system for potential fiber optic application. Materials Chemistry and Physics, 259, 123992.

Pal Singh, G., Kaur, P., Kaur, S., & Singh, D. P. (2011). Role of WO3 in structural and optical properties of WO3–Al2O3–PbO–B2O3 glasses. Physica B: Condensed Matter, 406(24), 4652–4656.

Palanivelu, N., & Rajendran, V. (2006, July 21). Dependence of elastic properties and ultrasonic velocities on the structure of vanadate lead tellurite glasses. Wiley Online Library.

Plucinski, M., & Zwanziger, J. W. (2015). Topological constraints and the Makishima–Mackenzie model. *Journal of Non-Crystalline Solids*, *429*, 20–23.

Plucinski, M., & Zwanziger, J. W. (2015). Topological constraints and the Makishima–Mackenzie model. Journal of Non-Crystalline Solids, 429, 20–23.

R. Christensen, J. Byer, T. Kaufmann and S.W. Martin, Structure-property relationships in the mixed glass former system Na2O-B2O3-P2O5, Physics and Chemistry of Glassess: European Journal of Glass Science and Technology, Part B, 50 (4), 237-242 (2009)

Saini, B., & Kaur, R. (2021). X-ray diffraction. Handbook of Modern Coating Technologies, 85–141.

Shi, Y., Tandia, A., Deng, B., Elliott, S. R., & Bauchy, M. (2020). Revisiting the Makishima–Mackenzie model for predicting the young's modulus of oxide glasses. *Acta Materialia*, *195*, 252–262.

Sponsored by Mo-Sci Corp.Feb 6 2020. (2020, May 12). Changing Glass Properties with Glass Modifiers. AZoM.com. https://www.azom.com/article.aspx?ArticleID=18872.

S, J. E. (1952). Tellurite Glasses. Nature, 169(4301), 581–582.

Structure and Density of Glass. (n.d.). http://www.eng.uc.edu/~beaucag/Classes/Properties/Polymer%20Textbook.pdf.

Tafida, R. A., Halimah, M. K., Muhammad, F. D., Chan, K. T., Onimisi, M. Y., Usman, A., Hamza, A. M., & Umar, S. A. (2020). Structural, optical and elastic properties of silver oxide incorporated zinc tellurite glass system doped with Sm3+ ions. Materials Chemistry and Physics, 246, 122801.

The Editors of Encyclopaedia Britannica. (2021, May 6). glass | Definition, Composition, Material, Types, & Facts. Encyclopedia Britannica. Retrieved from https://www.britannica.com/technology/glass

Titus, D., James Jebaseelan Samuel, E., & Roopan, S. M. (2019). Nanoparticle characterization techniques. Green Synthesis, Characterization and Applications of Nanoparticles, 303–319.

Umar, S. A., & Ibrahim, G. G. (n.d.). Theoretical Elastic Moduli of TeO2 – B2O3 – SiO2 Glasses. EDUCATUM Journal of Science, Mathematics and Technology. Retrieved from https://ejournal.upsi.edu.my/index.php/EJSMT/article/view/4013.

Vishwakarma, V., & Uthaman, S. (2020). *Environmental impact of sustainable green concrete*. X-ray Difraction.Retrieved from https://www.sciencedirect.com/topics/materials-science/x-ray-diffraction .

Zaid, Matori, Wah, Sidek, Halimah, Wahab, & Azmi. (2011). Elastic moduli prediction and correlation in soda lime silicate glasses containing ZnO, 1404–1410.

Zaki, M. R., Hamani, D., Dutreilh-Colas, M., Duclère, J.-R., de Clermont-Gallerande, J., Hayakawa, T., Masson, O., & Thomas, P. (2019). Structural investigation of new tellurite glasses belonging to the TeO2-NbO2.5-WO3 system, and a study of their linear and nonlinear optical properties. Journal of Non-Crystalline Solids, 512, 161–173.